NUMERICAL MODELING OF THE 3 FEBRUARY 2002 ÇAY EARTHQUAKE: GROUND MOTION SIMULATION AND INTENSITY DISTRIBUTION

A THESIS SUBMITTED TO
THE GRADUATE SCHOOL OF NATURAL AND APPLIED SCIENCES
OF
MIDDLE EAST TECHNICAL UNIVERSITY

BY

GİZEM CAN

IN PARTIAL FULFILLMENT OF THE REQUIREMENTS
FOR
THE DEGREE OF MASTER OF SCIENCE
IN
CIVIL ENGINEERING

APRIL, 2014

Approval of the thesis:

NUMERICAL MODELING OF 03 FEBRUARY ÇAY EARTHQUAKE: GROUND MOTION SIMULATION AND INTENSITY DISTRIBUTION

submitted by **GİZEM CAN** in partial fulfilment of the requirements for the degree **of Master of Science in Civil Engineering Department, Middle East Technical University** by,

Prof. Dr. Canan Özgen _____
Dean, Graduate School of **Natural and Applied Sciences**

Prof. Dr. Ahmet Cevdet Yalçıner _____
Head of Department, **Civil Engineering**

Assoc. Prof. Dr. Ayşegül Askan Gündoğan _____
Supervisor, **Civil Engineering Dept., METU**

Examining Committee Members:

Prof. Dr. Haluk Sucuoğlu _____
Civil Engineering Dept., METU

Assoc. Prof. Dr. Ayşegül Askan Gündoğan _____
Civil Engineering Dept., METU

Prof. Dr. Kemal Önder Çetin _____
Civil Engineering Dept., METU

Prof. Dr. H. Şebnem DÜZGÜN _____
Mining Engineering Dept., METU

Assoc. Prof. Dr. M. Altuğ Erberik _____
Civil Engineering Dept., METU

DATE :_____

I hereby declare that all information in this document has been obtained and presented in accordance with academic rules and ethical conduct. I also declare that, as required by these rules and conduct, I have fully cited and referenced all material and results that are not original to this work.

Name, Last Name: Gizem CAN

Signature:

ABSTRACT

NUMERICAL MODELING OF 3 FEBRUARY 2002 ÇAY EARTHQUAKE: GROUND MOTION SIMULATION AND INTENSITY DISTRIBUTION

Can, Gizem

M. Sc., Department of Civil Engineering

Supervisor: Assoc. Prof. Dr. Ayşegül Askan Gündoğan

April 2014, 78 pages

In seismically active regions strong ground motion estimation is essential for several purposes ranging from seismic design and analyses to disaster management. In regions of sparse seismic networks or seismic activity with long return periods, simulations become essential. This is particularly true when not only the peak ground motion parameters but the full time series of acceleration is required for earthquake engineering purposes. These simulations provide not only the earthquake engineering parameters but also give insight into the source, path and site effects observed during earthquakes.

In this study, 3 February 2002 Çay earthquake is simulated with the stochastic finite-fault method. This mainshock could only be recorded at four strong ground motion stations within an epicentral distance of 200 km. Thus, first it is aimed to simulate these sparse records and validate the simulation parameters at the stations. Then, a regional prediction of potential ground motions that occurred during the mainshock is generated. Finally, through an empirical relationship proposed for Turkey, a simulated intensity distribution is also obtained and compared to the observed intensity and damage data.

The results indicate that the mainshock is simulated effectively. This study and similar studies can be further developed and employed to assess potential ground motions in anticipated earthquakes such that necessary measures can be taken prior to large events to minimize future seismic losses in general.

Keywords: Earthquake, Strong ground motion simulation, Stochastic method, Finite-fault

ÖZ

3 ŞUBAT 2002 ÇAY DEPREMİNİN SAYISAL MODELLENMESİ: KUVVETLİ YER HAREKETİ SİMULASYONU VE EŞ ŞİDDET EĞRİSİ DAĞILIMI

Can, Gizem

Yüksek Lisans, İnşaat Mühendisliği Bölümü

Tez Yöneticisi: Doç. Dr. Ayşegül Askan Gündoğan

Nisan 2014, 78 sayfa

Sismik olarak aktif bölgelerde kuvvetli yer hareketlerinin belirlenmesi sismik tasarım ve analizden afet yönetimine dek uzanan çeşitli amaçlar için gereklidir. Az sayıda veri olan alanlar ile uzun tekerrür periyodu olan depremler içeren bölgelerde simülasyonlar önem kazanmaktadır. Bu durum özellikle yalnızca maksimum yer hareketi parametreleri gerektiğinde değil, deprem mühendisliği açısından tüm ivme-zaman kaydı talep edildiğinde geçerli olur. Simülasyonlar, yalnızca deprem mühendisliği parametreleri sağlamakla kalmaz; depremin kaynak, yayılım ve saha etkilerine de açıklık kazandırırlar.

Bu çalışmada, 3 Şubat 2002 Çay depremi stokastik sonlu-fay metodu ile simüle edilmiştir. Bu depremin anaşoku 200 km dışmerkezi mesafe içerisinde yalnızca dört istasyonda kaydedilebilmiştir. Bu çalışmada öncelikle bu kayıtlar simüle edilerek girdi parametreleri doğrulanmıştır. Daha sonra potansiyel yer hareketlerinin bölgesel dağılımı elde edilmiştir. Sonunda, Türkiye için önerilmiş olan bir ampirik denklem aracılığı ile simüle edilmiş şiddet haritası, deprem sonrası sahada gözlemlenmiş eşşiddet haritası ve hasar dağılımları ile karşılaştırılmıştır.

Sonuçlar, depremin etkili bir biçimde simüle edildiğini göstermektedir. Bu ve benzeri çalışmalar ileride geliştirilebilecek ve olası gelecek depremlerde ortaya

çıkabilecek potansiyel yer hareketleri henüz bu depremler olmadan değerlendirilip, gerekli hasar azaltma önlemleri alınabilecektir.

Anahtar Kelimeler: Deprem, Kuvvetli yer hareketi simülasyonu, Stokastik yöntem, Sonlu-fay

To my family

To my advisor

To my friends

ACKNOWLEDGEMENTS

I would like to express my sincere gratitude to my supervisor Assoc. Prof. Dr. Ayşegül Askan Gündoğan without her support and encouragement I could not complete my thesis successfully. It was a great honour to study my thesis with her from the beginning till the end. Especially, when the times I feel worried, she always encouraged and motivated me and never let me gave up. I am very fortunate to have an adviser who always make me smile.

I would also like to present my truthful thanks to Dr. Erhan Karaesmen and Dr. Engin Karaesmen. They always believed and supported me throughout my academic life, I hope I never make them disappointed.

I would like to show my true appreciate to Prof. Dr. Güney Özcebe. Without his guidance and moral support, the completion of this master study would be really difficult.

My next sincere gratitude is to Prof. Dr. Kemal Önder Çetin. His advices and encouragement always helped me for both my engineering and academic career. Working with him was a great pleasure in my undergraduate period.

I would like to thank my best friends Makbule Ilgaç and Ezgi Eroğlu. Without their friendship, this school would be so meaningless. What we did together always makes me happy, and I am very thankful that I have you in my life as my sisters.

My next appreciation goes to Özde Demirtürk. The distance does not separate a true friendship, and our relation is a proof of it, but I hope it does not last for a long time.

I would also like to express thanks to my friends, Kağan Erkek, Tamer Yetişir, Yağız Efe Bayiz, Aykut Demirel, Tuğçe Vural, Duygu Başar, Aytek Güven, Görkem Deniz Köksoy, Açelya Ecem Yıldız, Burak Akbaş, Semih Akkerman, Murat Altun and Semih Koç. I am really lucky that I have friends like you in my life.

My special thanks goes to Mustafa Bilal. His support and friendship throughout this study made my work easier and more enjoyable. Without his support, things would

be complicated. I would also like to thank all the members of A-team, especially to Barış Ünal, Nurten Şişman and Shaghayegh Karimzadeh.

This Master Study started in a small but lovely city of Italy, Pavia. Thanks to the programme, in a short period I gained invaluable friends of my life. I am so grateful to have friends all over the world, and I would like to thank both the men and kitchen team, Kathy Sassun, Yenshin Chen, Evangelia Batsi, Claudia Melania Pop, Sreeram Reddy Kotha, Andrea Spillatura, Giorgio Negrisoli, Francisco Figueroa, Danilo Tarquini, Yadong Jiang, Andrea Piazza, Dimitru Beilic, Semih Turkaya and Uğurcan Özçamur.

I would also like to thank Sevgi and Ali Güney Özcebe. I can never forget their encouragement they provided at the beginning of this my master study.

I want to thank to all my relatives. I am a big fan of this huge family who make me feel valuable. You are the treasure of my life, thank you for everything we shared.

Last but not least, I would like the express my greatest gratitude to the most valuable members of my life. My beloved mother Nuriye Can, father İbrahim Can and sister Sinem Can and my grandmother Armağan Altınkaya for their endless love, support and patience and not only for this study but also for my entire life.

TABLE OF CONTENTS

LIST OF TABLES

TABLES

LIST OF FIGURES

FIGURES

CHAPTER 1

INTRODUCTION

1.1 General

Considering the rate of occurrence and damage potential in terms of social and structural aspects they carry, earthquakes are among the most catastrophic natural hazards. Earthquake-related research is not only a major focus area in civil engineering, but also a multidisciplinary subject that involves researchers from earth sciences to structural engineering; from insurance industry to public policy.

The fundamental objective of studying earthquakes in structural engineering is to estimate the seismic loads to which a structure will be exposed during its lifetime. For this reason, ground motions are investigated in terms of their critical properties: amplitude, frequency content and duration. In regions where there is significant activity and dense seismic networks, it is possible to use real ground motion records for engineering purposes. When regional records are sparse, real records from other regions with similar tectonics and site conditions are mostly used. However, it is hard to find two locations on Earth with identical physical properties. Thus, simulated ground motions become a strong option in seismically active regions without abundant records or in regions that experience large earthquakes with longer return periods.

Empirical estimates of peak ground motion parameters as a function of magnitude, source-to-site distance and site conditions can be obtained from empirical Ground Motion Prediction Equations (GMPEs)- formerly recognized as attenuation

relationships. When the full waveform is required with its entire time history for engineering purposes, ground motion simulations become vital in regions of sparse data. In such cases, GMPEs are known to possess larger uncertainties, since these equations are derived from records of other areas with dense data. Another advantage of ground motion simulations is the ability to include the local site effects by modelling amplification through the shallow soil layers at a site of interest.

Almost all strong ground motion records are broadband records that include both low (<1 Hz) and high (>1 Hz) frequencies. Ground motion simulation methods vary in terms of their solution procedure for modelling these frequency bands. Mostly, deterministic approaches are used for simulating low frequencies while stochastic approaches are used for the higher frequencies. Full wave propagation methods are the most physical deterministic methods, however they are limited only up to some frequency levels since they require well-refined wave velocity models and an enormous computing power for broadband simulations. Stochastic methods on the other hand, are less accurate for not including the full propagation effects but they are very powerful in terms of practically modelling the intermediate to higher frequencies that mostly affect the building structures. The best option, whenever possible, is to use hybrid methods that combine deterministic and stochastic approaches in order to obtain realistic amplitudes over broadband frequency content.

In this study, 3 February 2002 Çay earthquake is simulated with the stochastic finite-fault method. This mainshock could only be recorded at four strong ground motion stations within an epicentral distance of 200 km. Thus, first it is aimed to simulate these sparse records and validate the simulation parameters at the stations. Then, a regional prediction of potential ground motions that occurred during the mainshock is generated. Finally, through an empirical relationship proposed for Turkey, a simulated intensity distribution is also obtained and compared to the observed intensity and damage data.

Since no refined wave velocity models exist for the region, lower frequencies are also considered within the stochastic technique. For reliable results, parameters are either adopted from previous studies or derived within this study.

1.2 Literature Survey

Ground motion simulation studies are at the centre of two disciplines: earth sciences and engineering. While engineers require and study simulated ground motions for the purposes stated previously, earth scientists study modelling of earthquakes to understand source, path and site effects better. But both have a common secondary objective: to estimate the anticipated ground motions during earthquakes at locations other than stations.

Time histories of ground motions using stochastic strong ground motion approach was first developed by superposing random amplitudes and duration with random time delays (Housner, 1947; Housner, 1955; Thomson, 1959). Then, the original method is improved by the further studies of Aki (1967) where the earthquake induced displacement is defined as a ramp function of time and correlated to the velocity function and source spectrum. Although there are several related studies (e.g.: Brune, 1970; Hanks, 1979), it is observed from seismologic evidence that the approach of Aki (1967) is the most physical model for estimating the high frequency portion of the earthquake records. In this model, a decrease of the amplitudes of the source spectrum proportional to the square of frequency (w^{-2} model) is observed.

Later, an improvement on the original ground motion model is made as follows: an earthquake record is represented as an event that is stochastic in time, with a Fourier amplitude spectrum specified fundamentally by seismological models of the source, path and site effects in a simple and deterministic way (Hanks and McGuire, 1981; Boore 1983, Silva 1991). Boore (1983) later combined the source spectrum of Aki (1967) and Brune (1971) with the findings of Hanks and McGuire (1981) and

proposed a methodology for generating time-domain simulations of ground motion records. In that method the fault is represented as a stochastic point-source. Later, Beresnev and Atkinson (1997) applied this methodology to model finite-faults. In their model, the fault plane is divided into smaller subfaults each of which is modeled as a point source. Then, by summing up the effects of these subfaults the overall radiation of motion from the whole fault can be established. The stochastic finite-fault methodology is further developed by Motazedian and Atkinson (2005) with a dynamic corner frequency approach which minimized the subfault dependency of the amplitudes in the simulation model.

Stochastic model is validated by several studies worldwide. Hanks and Boore (1984), Atkinson and Silva (2000), Motazedian and Atkinson (2005) worked on Californian events and validated the method within a region of abundant data. Recently, studies from Iran (e.g.: Motazedian and Moinfar, 2006; Shoja-Taheri and Ghofrani, 2007), Italy (e.g.: Castro *et al.* 2008; Galuzzo *et al.*, 2008; Ugurhan et al., 2012), Greece (e.g.: Roumelioti *et al.*, 2004) are also increasing in number. In Turkey, stochastic method has been used in several studies for validation of 1998 Ceyhan (Yalcinkaya, 2005), 1999 Düzce (Ugurhan and Askan, 2010) and 1992 Erzincan (Askan et al., 2013) earthquakes.

In this study, simulation of shear wave portion of the ground motion acceleration records from the 3 February Çay (M_w=6.6) earthquake measured at the near-field stations are simulated. The method followed is the stochastic finite fault method based on a dynamic corner frequency as introduced in Motazedian and Atkinson (2005).

1.3 Objective and Scope

The fundamental objective of this thesis is to assess the ground motion distribution of the 3 February Çay (M_w=6.6) earthquake in comparison with the observed intensity and damage distributions. For this purpose, initially the mainshock is simulated at the

limited number of stations available to validate the simulation input parameters. After validation, a blind simulation of the event is performed to obtain the anticipated ground motions at locations where there are no stations.

In Chapter 2, the basics of stochastic point source and finite-fault methodologies are described with the introduction of the parameters that are employed in the simulations. The alternative approaches taken in the definition of the corner frequencies are also discussed.

In Chapter 3, the 3 February 2002 Çay Earthquake is studied. Background information on the event and recorded strong ground motion data is presented. Then, stochastic finite-fault method is applied to verify regional seismic parameters through comparison of the synthetics with the real records of the Çay Earthquake's mainshock. Then, using those verified input parameters, a regional blind simulation is performed to obtain full ground motion time histories at locations where there are no strong motion records (dummy stations). The attenuation of the peak ground motion parameters at these nodes are first compared to the existing ground motion prediction equations. Then, these peak ground motion parameters are converted into felt intensity values and compared to the observed intensity and damage distributions.

In Chapter 4, a summary and conclusions of the thesis is presented with recommendations for further studies in this area.

CHAPTER 2

STOCHASTIC STRONG GROUND MOTION SIMULATION METHODOLOGY

2.1 General

In this part of the study, method for strong ground motion simulation of Çay Earthquake is described. Theory beneath the simulation methodology, comparison of stochastic point-source and finite-fault models, and factors affecting the simulation are presented in the following subsections. In this method, the individual characteristics of seismic source, path (propagation) effects, and local site conditions are taken into account in the frequency domain, when generating synthetic ground motions.

The fundamental output of the stochastic ground motion simulation methodology is the acceleration time history and Fourier Amplitude spectrum is at the free field for a given set of source, path and local site conditions.

In Section 2.2, stochastic point source modeling is described with details of source, path and site parameters as described in subsections 2.2.1, 2.2.2 and 2.2.3, respectively. In Section 2.3, the methodology is extended from point-sources to finite-faults. In addition, different definitions of the corner frequency are provided.

2.2 Stochastic Point Source Modeling

From engineering point of view, main concern of ground motion analyses is the damage potential of the strong ground motion. In that perspective, the influence of the duration and amplitudes of intermediate to high frequency portion of the records should be investigated. However, due to the complex phase behaviour of the high frequency range of the motion, deterministic simulation technique is not the best way to model frequencies greater than 1 Hz. In the stochastic simulation method, based on the randomness in the energy dispersion of the source, much data from previous events worldwide is simulated effectively. Time-domain measures such as peak acceleration and peak velocity, short period P- and S- wave amplitudes as well as frequency domain measures such as Fourier Amplitude Spectrum (FAS) have been predicted with reasonable accuracy through this method (Hanks and McGuire, 1981; Boore, 1983; Boore and Atkinson, 1987; Silva and Lee, 1987; Toro and McGuire, 1987).

Theoretical predictions of seismic motions as a function of seismic source strength are often expressed as frequency-domain scaling models. The measures of interest in strong-motion seismology, however, are usually in the time domain. The stochastic method makes use of both domains; its essence is to filter a suite of windowed, stochastic time series so that the amplitude spectra are equal, on the average, to a specified deterministic spectra. Its success in predicting peak accelerations (Hanks and McGuire, 1981) is mostly due to the w^{-2}squared spectrum with a high-frequency cut-off of Aki (1967).

After the initial development of stochastic time series, Boore (1983) introduced a method for generating S-wave portion of the seismic waves due to point-sources. That algorithm is based on the original findings of Hanks and McGuire (1981) who showed that high-frequency ground motion of shear-waves can be represented as finite duration, band-limited, white Gaussian noise. The basic aim of the simulation methodology is to generate a transient time series whose amplitude spectrum is the

theoretical deterministic spectrum obtained from wave propagation solutions in the homogeneous half space.

The idea is to generate a time series of filtered and windowed Gaussian white noise whose amplitude spectrum approximates the acceleration spectrum given by physical considerations- in this case the Brune (1970) spectrum modified to remove frequencies above a certain cut-off frequency. With a prescribed stress parameter (stress drop), the scaling with earthquake size at a given distance depends on only one parameter-seismic moment (or equivalently, moment magnitude). This simple one-parameter scaling model provides a good approximation to many measures of high-frequency strong ground motion based on analysis of hundreds of strong-motion recordings.

The algorithm of stochastic point-source modeling of strong ground motions starts with the windowing of a time sequence of band-limited random Gaussian noise with zero expected mean and variance chosen to give unit spectral amplitude on the average. Then, the generated noise is windowed to give a pyhsical shape of an acceleration-time series. The types of windows generally used for this purpose are Saragoni-Hart and boxcar windows. Saragoni and Hart (1974) found that this window is a good representation of the averaged envelope of the squared acceleration time series. The spectrum of the windowed time series is then multiplied by the theoretical deterministic S-wave spectrum. Finally, the transformation back to time domain yields the final time series (Boore, 2003). The product of filter functions representing source (E), propagation (P), and site effects (G), and the instrument response (I), results in the Fourier Amplitude Spectrum of a seismic signal given as:

$$A(M_0, R, w) = E(M_0, w)P(R, w)G(w)I(w) \tag{2.1}$$

where M_0 is the seismic moment, w is the frequency, R is the source to site distance. The flowchart of the algorithm is outlined in Figure 2.1.

2.2.1 Source Effects

Source models usually involve a kinematic rupture process on a fault plane with specified dimensions and orientation whose physical properties, such as slip or rupture velocity, vary randomly over the fault surface (e.g., Bouchon, 1978; Joyner and Boore, 1980). More complex source models are the ones that involve dynamic rupture on the fault: they are more physical but require more information on the source complexity and significant computational effort.

The derivation of the source function in stochastic modeling starts with the solution of the elastodynamic wave equation expressed in its most general form as follows:

$$\rho \frac{\partial^2}{t^2} u(x,t) = (\lambda + \mu)\nabla\big(\nabla \cdot u(x,t)\big) + \mu\nabla^2 u(x,t) + f(x,t) \qquad (2.2)$$

where $u(x,t)$ is the particle displacement; ρ is the crustal density; λ and μ are the elastic constants from which P- and S-wave velocities are defined as $\alpha = \sqrt{\frac{(\lambda+2\mu)}{\rho}}$ and $\beta = \sqrt{\frac{(\mu)}{\rho}}$. Here f(x, t) is the dynamic forcing function.

Green's function solution for the far-field shear wave displacement in a homogeneous, isotropic, unbounded medium due to a point shear dislocation is expressed in time domain as follows:

$$u(x,t) = \frac{\Re^{\theta\gamma}}{4\pi\rho\beta^3 R} M'(t)\left(t - \frac{R}{\beta}\right) \qquad (2.3)$$

where $u(x,t)$ is the dynamic displacement field at point x, $\Re^{\theta\gamma}$ is the radiation pattern reflecting the variation of the displacement field for different directions due to a shear dislocation, β is the shear-wave velocity, R is the source to receiver distance and $M'(t)$ is the moment rate function which is the time derivative of the seismic moment $M(t)$ as defined in Aki and Richards (1980):

$$M(t) = \mu \bar{u}(t) A \tag{2.4}$$

where μ is the shear modulus or rigidity, $\bar{u}(t)$ is the source time function and A is the dislocation area.

Source time function represents the dynamic change in the amplitude of forcing function $f(x,t)$ on the fault plane. It is one of the uncertain parameters describing the source. Aki (1967) utilized a step function to represent the increase of particle displacements with time while Haskell (1964) assumed a ramp function.

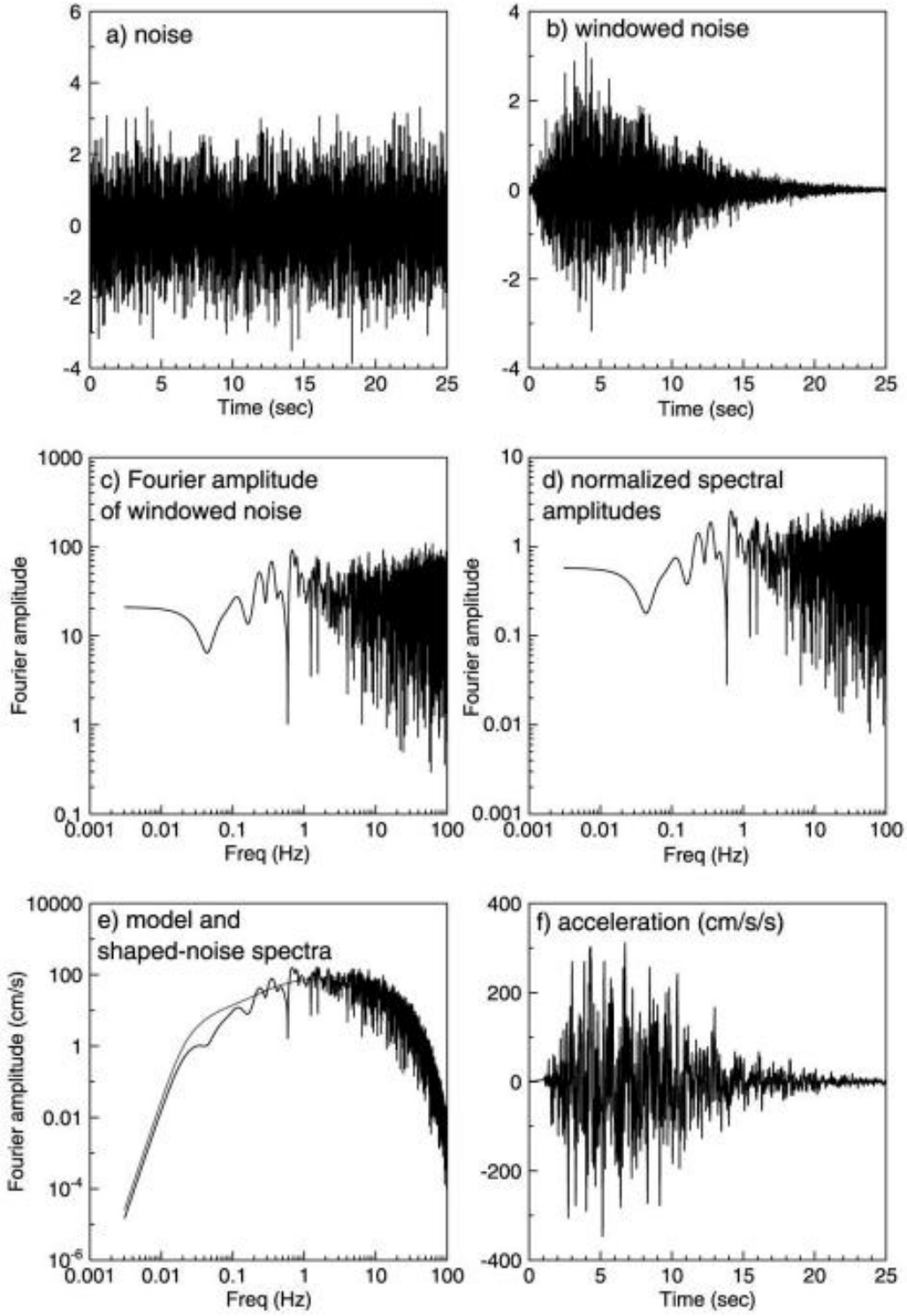

Figure 2.1: The main steps of stochastic strong ground motion method (adapted from Boore, 2003)

In stochastic modeling, the following source-time function is employed which is indeed a smoothed ramp function:

$$\bar{u}(t) = \frac{\sigma}{\mu}\beta\tau\left[1 - \left(1 + \frac{t}{\tau}\right)e^{-\frac{t}{\tau}}\right] \tag{2.5}$$

where the derivative becomes:

$$\bar{u}'^{(t)} = \frac{\sigma}{\mu}\beta\left(\frac{t}{\tau}\right)\left(e^{-\frac{t}{\tau}}\right) \tag{2.6}$$

Thus, Equation (2.3) becomes:

$$u(x,t) = \frac{\Re^{\theta\gamma}M_0}{4\pi\rho\beta^3 R\tau}\left(\frac{t-\frac{R}{\beta}}{\tau}\right)e^{-\frac{\left[t-\frac{R}{\beta}\right]}{\tau}} \tag{2.7}$$

Since stochastic modeling works in the frequency domain, Fourier transformation is required which then leads to:

$$u(x,\omega) = \frac{\Re^{\theta\gamma}M_0}{4\pi\rho\beta^3 R}\left[\frac{1}{1 + \left(\frac{\omega}{\omega_c}\right)^2}\right] \tag{2.8}$$

Here the corner frequency ($f_c = \omega_c/2\pi$) is defined as:

$$f_c = 4.9 \times 10^6 \beta\left(\frac{\Delta\sigma}{M_0}\right)^{1/3} \tag{2.9}$$

where f_c is in Hertz (Hz), shear-wave velocity β is in km/sec, stress drop $\Delta\sigma$ is in bars and the seismic moment M_0 is in dyne·cm.

To summarize, the general form of the source function in terms of constants C, seismic moment and source displacement spectrum is expressed as follows:

$$E(M_0, \omega) = CM_0S(\omega, \omega_c) \tag{2.10}$$

where C is the combined form of the constants defined in Equation (2.11), or:

$$C = \frac{\Re^{\theta\gamma} \cdot FS \cdot PRTITN}{4\pi\rho\beta^3} \tag{2.11}$$

Here, FS is the free surface amplification factor whose value is generally assumed to be 2. $PRTITN$ is a factor applied to reflect the effect of shear-wave energy partitioning into two horizontal components and its value is generally assumed to be $1/\sqrt{2}$. The radiation pattern constant $\Re^{\theta\gamma}$ is mostly taken as 0.55 for shear waves.

Lastly, the source displacement spectrum (ω^{-2} spectrum) is defined as:

$$S(\omega, \omega_c) = \frac{1}{1 + \left(\frac{\omega}{\omega_c}\right)^2} \tag{2.12}$$

It must be noted that despite all the measures taken to physically model the source processes, the weakest part of the stochastic modeling is still the source definitions which does not fully include complex source behaviour. For this reason, stochastic models are observed to work only limitedly for the lower frequencies which are most affected from the source effects during large earthquakes (Askan et al., 2013). Luckily, the frequencies of engineering interest (other than very flexible structures) do not lie within this low frequency band, which makes simulated ground motions useful for engineering purposes.

2.2.2 Path Effects

There are three main parameters of the strong ground motion: amplitudes, frequency content and duration. Path effects basically involve the wave propagation through

deeper layers in the Earth which can be described with three major parameters, geometric spreading, quality factor (anelastic attenuation term) and duration.

As the waves travel through the Earth, the amplitudes of the ground motions are reduced with distance by a factor defined as geometric spreading. In case of only body waves in homogeneous media, this factor is simply 1/R where R is the distance from the source. However, since real Earth is heterogeneous in structure, geometrical spreading in some regions is different. In such cases, geometric spreading term should be selected or derived considering the regional dataset that is available. There are also global definitions derived from worldwide data that could be used for similar seismotectonics.

The next important parameter is anelastic attenuation term (or the quality factor). Different than the geometric spreading factor, quality term is related to the anelastic losses in Earth material where some of the energy that is released by the earthquake is damped during wave propagation. Since every seismic region in the Earth have different damping characteristics, a corresponding quality function should be selected, in case there is one in the literature (Aki, 1980). Otherwise, quality factor models can be derived with a large set of regional seismic data. Frequency-dependent quality factor term can be represented as follows:

$$Q = Q_0 f^n \tag{2.13}$$

where Q_0 is related to heterogeneous behavior of Earth media and n is a region-dependent parameter (Raghukanth and Somala, 2009). In order to the get a proper estimation of the shape of the high frequency spectrum of ground motion, as explained in Motazedian (2006), quality factor is an important parameter.

In summary, the overall path effect on stochastic simulation of ground motions, considering both the geometric spreading and anelastic attenuation, can be represented as (Boore, 2003):

$$P(R, w) = Z(R) e^{-\frac{\pi f R}{Q(f)\beta}} \tag{2.14}$$

$$Z(R) = \begin{cases} \dfrac{R_0}{R}, & R \le R_1 \\ Z(R_1)\left(\dfrac{R_1}{R}\right)^{p_1}, & R_1 \le R \le R_2 \\ \vdots & \\ Z(R_n)\left(\dfrac{R_n}{R}\right)^{p_n}, & R \le R_n \end{cases} \tag{2.15}$$

where $Z(R)$ is the geometric spreading term and $e^{-\frac{\pi f R}{Q(f)\beta}}$ is the exponential decay function due to the anelastic attenuation. In both terms, R is the epicentral distance of the earthquake to the observation point.

Distance-dependent duration is the last parameter regarding the path effects while simulating the ground motion. Duration effects are physically observable in the seismograms of the same event. When different arrivals are observed in the seismograms, it is inferred that waves have taken different paths which are indicators of the scattering and multipathing processes (Stein and Wysession, 2003). These two processes have a similar effect of enhancing the duration of the waves.

Since full wave propagation is not performed within the stochastic method, the duration is expressed as an empirical function. The form of the duration function can be shown as:

$$T = T_0 + bR_{hypo} \tag{2.16}$$

where T_0 the source duration and b is the slope of distance-dependent duration term where R is the source to site distance (Beresnev and Atkinson, 1997).

Finally, determining regional models for geometric spreading, quality factor and duration effects are not a straightforward procedure. It requires large and reliable regional datasets. Comparison of synthetic and recorded ground motions provide a solid understanding to source and path properties; however it is an iterative procedure with potential trade-off between parameters. Optimal simulation parameters are generally determined by forward fitting of the FAS of the recorded motion by the FAS of the simulated ground motion.

2.2.3 Site Effects

One of the most important inputs of the stochastic modeling is the local site functions since the characteristics of strong ground motions are directly affected these frequency-dependent effects. In addition, site effects influence all of the main characteristics of the ground motion; amplitude, frequency content and duration. Since these properties strongly depend on the soil underneath, modeling of the profile should be carefully investigated.

Site effects are dependent on several factors: soil type, relative seismic impedance of soil layers, reflection and refraction processes of the propagating seismic waves through the soil media (which can either increase or decrease the wave amplitudes). Going from bedrock to the surface, density and velocity of soil layers generally vary. When waves travel up through the Earth, since the seismic impedance decreases, wave amplitudes must increase in order to conserve the elastic wave energy (Kramer, 1996). However, there is also the damping effect in the soft soil layers which can cause a counteracting decrease in wave amplitudes. Therefore, site effect is a combination of amplification and diminution factors which will be described in the next subsections.

An important point is the distinction between the site and path functions. Path effects basically involve the wave propagation through deeper layers in the Earth while site effects involve the shallow soil layers beneath the surface.

2.2.3.1 Amplification Function

For site amplification calculations, there are different methodologies depending on whether the velocity profile of the site is known or not. Amplification functions using site-specific velocity profiles yield more physical results; however determining velocity profiles with in-situ or theoretical procedures is mostly difficult and

expensive. Thus, other approximate empirical approaches for calculating amplification functions can be preferred in some cases.

The two common theoretical methods for estimating site amplifications are the theoretical site response analyses (Schnabel et al., 1972) and quarter wave length method (Boore and Joyner, 1997). On the other hand, the most commonly-used empirical method is the Horizontal to Vertical Spectral Ratio (HVSR or H/V) method introduced by Nakamura, (1989).

In quarter wavelength approach, the amplification factors for each frequency is defined as the ratio of seismic impedance at source level to the average seismic impedance corresponding to a specific depth (Boore and Joyner, 1997). The function is represented as:

$$A\big(f(z)\big) = \sqrt{\frac{\rho_s \beta_s}{\overline{\rho(z)}\,\bar{\beta}(z)}} \tag{2.17}$$

Boore and Joyner (1997) performed this method on representative soil profiles and obtained generic site amplification functions as a function of NEHRP soil type. In cases where there is no detailed site profile information at a site of interest, these generic amplification functions can be implemented despite their uncertainty.

The most common theoretical method for estimating site amplifications is the theoretical site response analyses (Schnabel et al., 1972). Even though it is possible to find amplifications based on complex 2-D (Sanchez-Sesma, 1987) or 3-D (Pitarka *et al.*, 1998) velocity models, the original method is derived on 1-D velocity profiles. It is applied in many studies due to its theoretical basis and simplicity. In this approach, the soil is modeled as a series of infinite horizontal layers on top of uniform half-space where the non-linear behavior of the soil is simulated with an equivalent linear analysis.

The input parameters required are thickness, density, wave velocity, shear modulus reduction and damping curves of each layer. The algorithm works in frequency

domain basically in the form of 1-D wave propagation though the soil layers (Kramer, 1996).

Its use is not recommended in ground motion modeling in sedimentary basins since a full basin effect must be studies with at least 2-D wave velocity models.

At sites without velocity profiles where theoretical methods cannot be used, an empirical approach by Nakamura (1989), H/V method is preferred. The H/V ratios (or HVSR spectra) are simply the ratios of the mean FAS of the horizontal components to that of the vertical component of an acceleration record in the frequency domain. The resulting spectrum is employed as a direct measure of amplification function. This method is fundamentally based on the fact that HVSR is closely related to Rayleigh wave ellipticity in a layered medium (e.g.: Lachet and Bard, 1994; Tokimatsu, 1997; Scherbaum et al., 2003). At S-wave resonance frequencies, the Rayleigh wave's elliptical motion tends to degenerate into predominately horizontal motion where HVSR yields a qualitative estimate of the natural resonance frequency of layered sediments (Claprood and Asten, 2009).

Practically, the H/V ratios assume that the horizontal component of ground motion is more exposed to amplification through the shallow soil layers than the vertical component. Thus, theoretical amplification factors can be approximated by dividing the Fourier Amplitude Spectrum of the horizontal ground motion to that of vertical ground motion as follows:

$$A(f) = \frac{FAS_H(f)}{FAS_V(f)} \tag{2.18}$$

At a site of interest, mean H/V ratio from an ensemble of high-quality strong motion records can be employed as the approximate amplification spectra. However, the results are almost always subjected to large uncertainties since datasets are rarely complete.

In this study, both empirical and theoretical site amplification functions are derived. Further explanation will be given in Chapter3.

2.2.3.2 Diminution Function

Under the effect of near field conditions, a rapid decay of the spectral values in the high-frequencies is observed. This diminution effect is not due to the attenuation during wave propagation (Boore, 1983). There are alternating views on whether this decay is fundamentally a source property, a site effect or a combination of both (Askan et al., 2014). Papageorgiou and Aki (1983) express that decrease in high frequencies is due to the source processes; on the other hand Hanks (1982) and Atkinson (2004) assign this condition to attenuation in near-surface soil layers.

There are two approaches to model this decay in high frequency portion of strong ground motion records: f_{max} and kappa. Among these two, f_{max} is represented as the cut-off frequency (Hanks, 1982) of the seismogram and the corresponding diminution factor is given as:

$$D(f) = \left(1 + \left(\frac{f}{f_{max}}\right)^{8}\right)^{-0.5} \tag{2.19}$$

Alternatively, the spectral decay at high frequencies is formulated with the kappa factor (κ) which is a site specific parameter illustrating the extent of near-surface attenuation mechanism. Thus, the spectral decay at high frequencies are introduced by Anderson and Hough (1984) as:

$$D(f) = e^{-\pi\kappa_0 f} \tag{2.20}$$

In this equation the parameters are defined as follows: The spectral decay at high frequencies is considered as an exponential function by Anderson and Hough (1984). For both horizontal and vertical ground motions, to estimate the corresponding kappa values, Fourier Amplitude Spectrum of each record is plotted in semi-logarithmic scale. Next, the frequencies where linear decay of log (Amplitudes) starts (f_e) and ends (f_x) are selected manually for each component. A linear fit yields the kappa values of that single record. However, this kappa value includes the distance-dependent attenuation (path) effects which must be removed thus a zero-distance

kappa value (κ_0) must be estimated in the region. For this purpose, kappa values from single records are plotted against the epicentral distances for each station separately. Through a linear regression to this data, the ordinate of the best-fit line provides the zero-distance kappa (κ_0) value for the region of interest.

2.3 Stochastic Finite-Fault Modeling

Finite-fault models are extensions of original point-source models. When the observation points are no longer at distances greater than the larger dimension of the fault plane, the method must be improved to model the finite-fault effects. To simulate these effects, the rectangular fault plane is divided into smaller subfaults each of which is treated as a stochastic point source. Then, by summing up the effects of these subfaults in time domain, the resulting accelerogram can be obtained (Beresnev and Atkinson, 1997). The idea of discretization of large events and superimposing the contribution of every small element in the discretized space was first introduced in the original work of Hartzell (1978).

Since the near-field effects is the main concern of stochastic finite-fault modeling, to represent the effect of a specified fault plane, an area of rupture is defined by assigning a finite rupture length and width. Contribution of each point source with an ω^{-2} spectrum to the total ground motion from that plane is summed with physically-appropriate time delays. To get the overall response at the observation point, the contribution and timing of every single source should be taken into account (Atkinson *et al.*, 2009). Following formula is used to get the ground motion acceleration at an observation point by summing up the contribution of each source along the length and width of rupture plane:

$$\mathrm{a(t)} = \sum_{i=1}^{nl} \sum_{j=1}^{nw} a_{ij}\left(t - \Delta t_{ij} - T_{ij}\right) \tag{2.21}$$

where a(t) is the ground motion acceleration from the entire fault whereas a_{ij} is the ground motion acceleration obtained from the ij^{th} subfault. Here, nl and nw are the number of subfaults along the length and width of main fault, respectively. T_{ij} is a fraction of rise time of a subfault where rise time is defined as the subfault radius divided by the rupture velocity (Atkinson *et al.*, 2009). The time delay for each element Δt_{ij}, is the summation of the time required for the rupture front to reach the element and the time required for the shear-wave to reach the receiver after the element has been triggered (Beresnev and Atkinson, 1997). The schematic distribution of the wavefront from the finite fault is displayed in Figure 2.0.2.

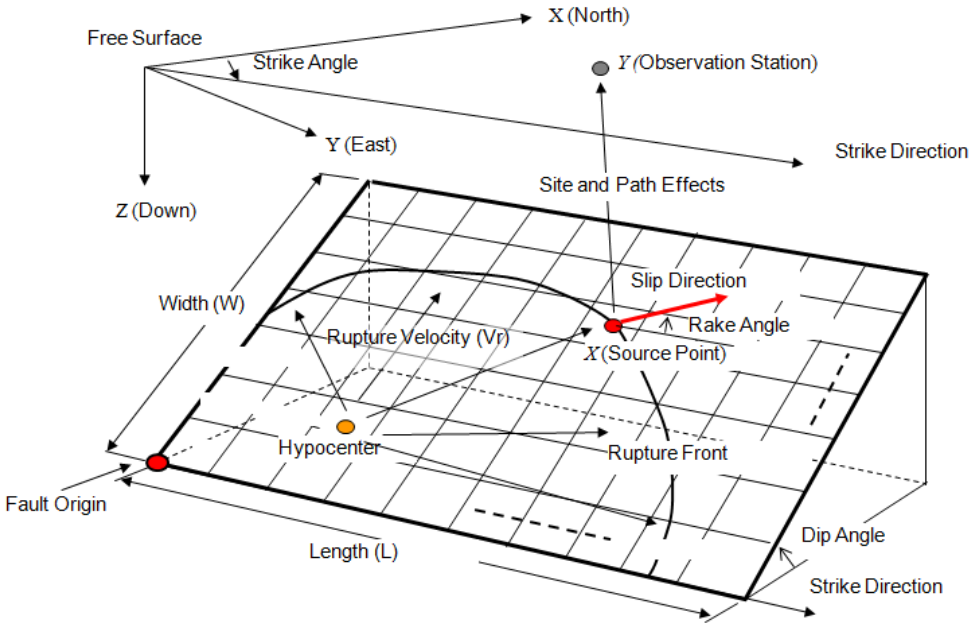

Figure 2.2: Wave propagation on a rectangular finite fault model (Adapted from Hisada, 2008)

When the distribution of slip values along the fault plane is assumed to be homogeneous, the moment of each subfault is defined as follows:

$$M_{0_{ij}} = \frac{M_0}{N} \tag{2.22}$$

where *N* is the number of subfaults, M_0 is the total seismic moment. If the subfaults are not identical, the distribution of the seismic moment among the subfaults is based on the slip weights (Motazedian and Moinfar, 2006). The moment of each subfault is then defined as:

$$a(t) = \frac{M_0 S_{ij}}{\sum_{k=1}^{nl} \sum_{l=1}^{nw} S_{kl}} \tag{2.23}$$

where S_{ij} is the relative slip weight of the ijth subfault.

In their early work, Beresnev and Atkinson (1997) defined the Fourier acceleration spectrum of a subfault ij, A_{ij} to be exactly the same with that of stochastic point-source:

$$A_{ij}(f) = \frac{CM_{0_{ij}}(2\pi f)^2}{1 + \left(\frac{f}{f_{c_{ij}}}\right)^2} \left(\frac{1}{R_{ij}}\right) e^{-\frac{\pi f R_{ij}}{Q\beta}} D(f) e^{-\pi\kappa f} \tag{2.24}$$

where the corner frequency of a subfault, f_{cij} is defined as:

$$f_{c_{ij}} = 4.9 * 10^6 \beta \left(\frac{\Delta\sigma}{M_{0_{ij}}}\right)^{\frac{1}{3}} \tag{2.25}$$

Remaining terms are the same as previously defined in this Chapter.

In the literature, the original program that used the stochastic finite-fault methodology was FINSIM (Beresnev and Atkinson, 1998a; 1998b). In order to overcome the dependency of the amplitudes and corner frequency of the synthetic ground motion on the number of subfaults and subfault size, the program is further developed by Motazedian and Atkinson (2005). The second program is named as EXSIM which improves the method outlined previously with a dynamic corner frequency. In this updated method, while the rupture propagates the corner frequency

changes inversely proportional to ruptured area at that time. The dynamic corner frequency is expressed as follows:

$$\mathrm{f_{c_{ij}}} = \mathrm{N_R(t)}^{-\frac{1}{3}}\, 4.9 * 10^6 \beta \left(\frac{\Delta\sigma}{M_{0_{ave}}}\right)^{\frac{1}{3}} \tag{2.26}$$

where $\mathrm{N_R}(t)$ is the cumulative number of ruptured subfaults at time t, $M_{0_{ave}} = M_0/N$ is the average seismic moment of subfaults.

In this new approach, since the ruptured area increases as the fault rupture progresses, to conserve the radiated energy at high frequencies that control the acceleration-sensitive region, a scaling factor $\mathrm{H_{ij}}$ is applied to the spectrum (Motazedian and Atkinson, 2005). The updated formulation of acceleration spectrum with the new scaling factor is defined as follows:

$$\mathrm{A_{ij}}(f) = \frac{C M_{0_{ij}} H_{ij} (2\pi f)^2}{1 + \left(\frac{f}{f_{c_{ij}}}\right)^2} \left(\frac{1}{R_{ij}}\right) e^{-\frac{\pi f R_{ij}}{Q\beta}} D(f) e^{-\pi\kappa f} \tag{2.27}$$

$$\mathrm{H_{ij}} = \left(N \frac{\sum \frac{f^2}{1 + \left(\frac{f}{f_c}\right)^2}^2}{\sum \frac{f^2}{1 + \left(\frac{f}{f_{ij}}\right)^2}^2} \right)^{\frac{1}{2}} \tag{2.28}$$

Dynamic corner frequency approach is not the only change in methodology updated by Motazedian and Atkinson (2005): An additional adjustment is the implementation of maximum ruptured area divided by the total fault area named as pulsing area percentage. Until pulsing area percentage is reached by subfaults, rupture on the fault propagates. Therefore, until pulsing percentage is attained, corner frequency decreases, since it is related to the ruptured area of subfaults as described previously.

It must be noted that the stochastic method yields only a single horizontal component of the ground motion. The motion is assumed to be independent of direction.

In this thesis, strong ground motion simulation of 3 February 2002 Çay earthquake using stochastic finite-fault methodology based on a dynamic corner frequency is employed. Chapter 3 presents the numerical values of the described input parameters and the results in detail.

CHAPTER 3

GROUND MOTION SIMULATION OF THE 3 FEBRUARY 2002 ÇAY EARTHQUAKE (M_w=6.6): A VALIDATION STUDY

3.1 General

In this chapter, stochastic strong ground motion simulation of the 3 February 2002 Çay earthquake at selected near fault stations is performed. Through this simulation, initially the regional seismic parameters are verified by comparing the synthetics with the real records of the Çay earthquake's mainshock. Then, using those verified input parameters, a regional blind simulation is performed to obtain full ground motion time histories at locations where there are no strong motion records. The attenuation of peak ground motion parameters at these nodes are first compared to the existing ground motion prediction equations. Finally, these peak ground motion parameters are converted into felt intensity values and compared to the observed intensity and damage distributions near the epicentral area.

In Section 3.2, background information on Çay earthquake and tectonics of the region is presented. In Section 3.3, strong motion records of the mainshock obtained at the near fault stations are investigated. The model parameters used in the simulations and their derivations (or adaptations) is discussed in Section 3.4. Later, in Section 3.5, simulation results at the stations are presented. In Section 3.6, blind simulations are performed at dummy stations located around the epicentral area.

Then, in subsection 3.6.1, first the spatial distribution of peak ground motion parameters in the meizoseismal area are presented. Then, attenuation of these synthetic peak amplitudes are compared with empirical ground motion prediction equations. Finally, in subsection 3.6.2, felt intensity values obtained from the synthetics are compared with the observed intensity and damage distributions.

3.2 Background Information

On 3 February 2002 at 09:11 with local Turkish time, an earthquake occurred near Çay town of Afyon city on the fault segment between Eber and Akşehir Lakes. When the distribution of damage and epicentral locations stated by different institutes are taken into account, the earthquake is named as ‘‘Çay-Eber Earthquake’’ (Ulusay et al., 2002). 42 people lost their lives due to this event and many buildings are damaged to various extents, of which the details will be given in Section 3.6.2.

The epicenter of the mainshock is located between Akşehir and Eber Lakes with an East-West orientation. Three major aftershocks occurred within a range of moment magnitude (M_w) 4.8-6.0 at 11:26, 13:39, and 13:54 in local time. Although the region seemed less active after year 1946; the 2000 Sultandağı Earthquake (M_w= 6.0) and the 2002 Çay Earthquake (Mw=6.6) is a proof of ongoing extension (Taymaz and Tan 2001; Utku et al. 2003).

The earthquake happened in a seismically active region of Central Anatolia, at the eastern bound of Western Anatolia and at the tip of the Isparta Angle (Akinci et.al, 2013). The affected area is bounded by Sultandağları and Emirdağları mountain ranges. The region of interest is at the junction of three depressions: Aksehir-Bolvadin, Çay-Afyon and Karadilli-Çay-Üçkuyu-Yunak (Karamık Graben).

Although the Sultandağı fault (located on the Akşehir Fault Zone) was earlier identified as a thrust fault (Boray et al.1985; Şaroğlu et al., 1987), recent geological research around the region (Kocyigit et al., 2000) proved that it is a normal fault dipping North-East with minor strike-slip component. Sultandağı fault is surrounded

by the Burdur-Dinar and Gediz-Simav regions. Tectonics of the region with historic as well as instrumental-era events and the corresponding aftershock activity can be seen in Figure 3.1 and Figure 3.2**,** respectively.

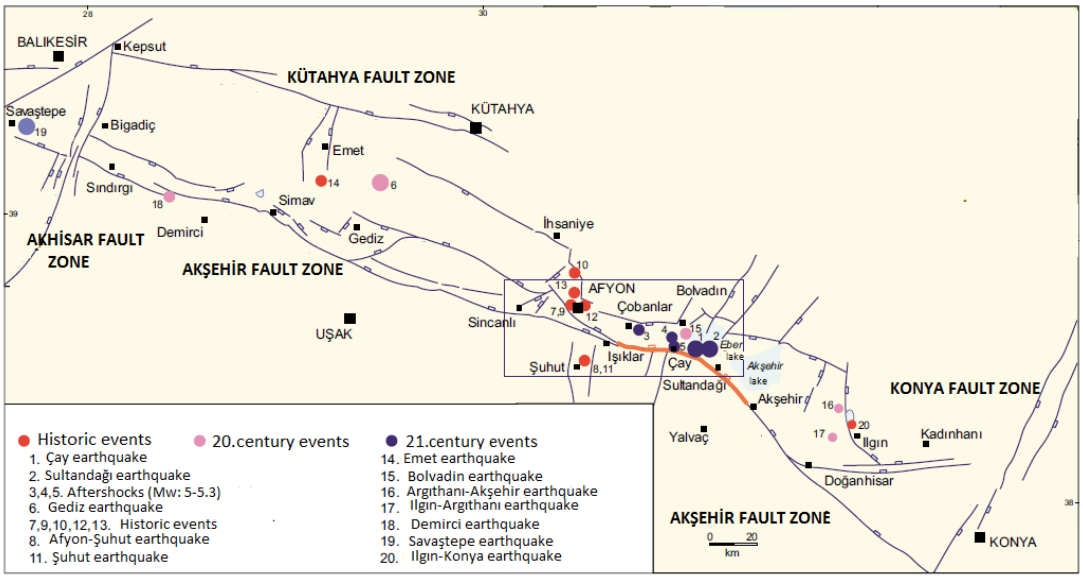

Figure 3.1: Historical and instrumental-era events in the near fault region of 2002 Çay earthquake (adapted from Kocyigit, 2002)

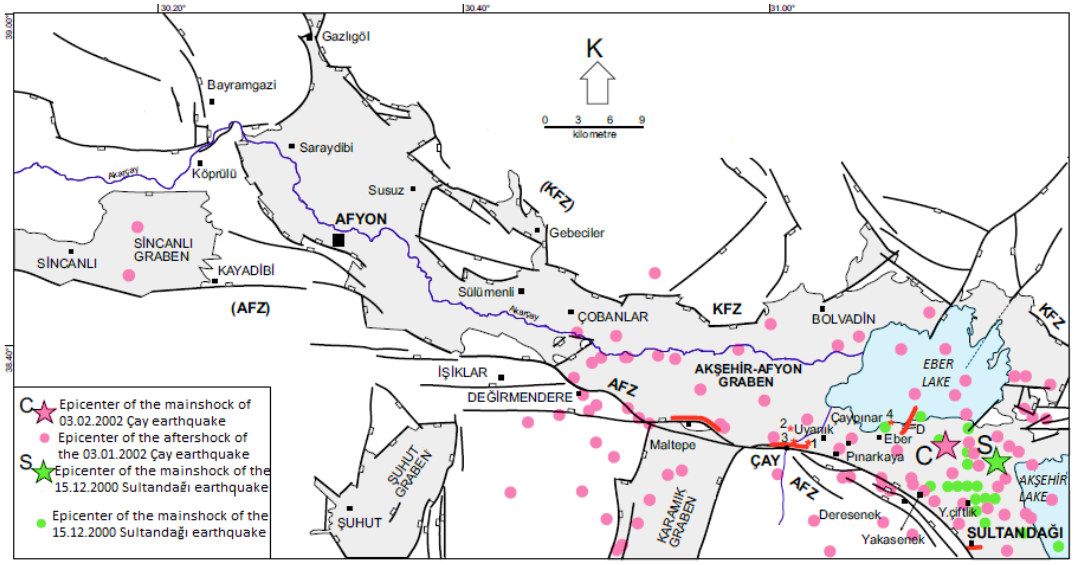

Figure 3.2: Aftershock activity in the near fault region of 2002 Çay earthquake (adapted from Kocyigit, 2002)

After the 3 February 2002 Çay Earthquake, source parameters and focal mechanism of the event is examined by different institutes and researchers. The results from USGS-NEIC (2002), ERI (2002), HARVARD (2002), EMSC (2002), ETHZ (2002) and KOERI (2002) showed that the mainshock is resulted by an almost pure normal faulting mechanism with minor strike slip constituent on a fault segment striking NE–SW (Aktuğ et.al,2009). The focal mechanisms of the earthquake from different institutions are shown on Figure 3.3. In this study, the model of Aktuğ (2009) is employed since it is consistent with the regional geologic evidence.

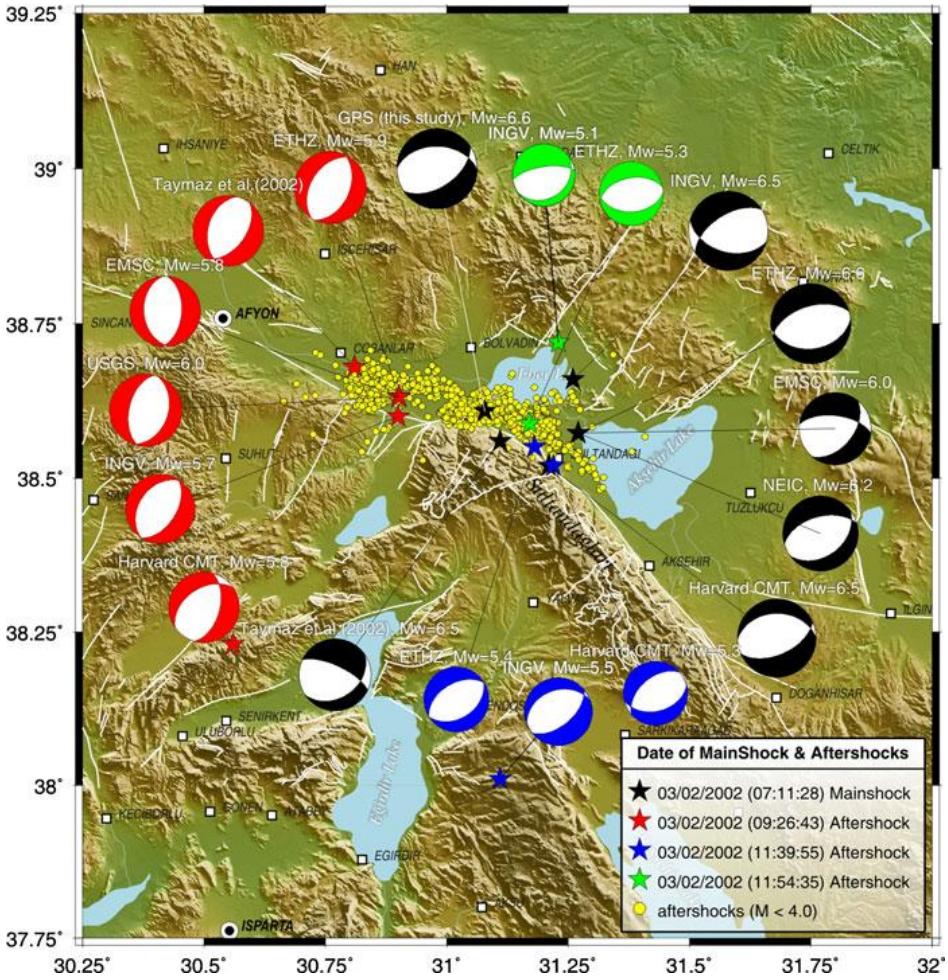

Figure 3.3: Focal Mechanism of the 3 February 2002 Çay earthquake by different institutes and researchers (adapted from Aktug, 2009)

3.3 Strong Ground Motion Data

3 February 2002 Çay earthquake is recorded by only six strong motion stations. The raw versions of the recorded strong ground motions are all taken from DAPHNE database via http://kyhdata.deprem.gov.tr/2K/kyhdata_v4.php. Location of strong ground motion stations that recorded the mainshock are shown in Figure 3.4. Since the far-field ground motions do not possess much significance in terms of damage potential of the event, in this study four stations within the epicentral distance of 200 km are selected. The stations of interest are the ones located in Afyon, Kütahya, Uşak and Burdur.

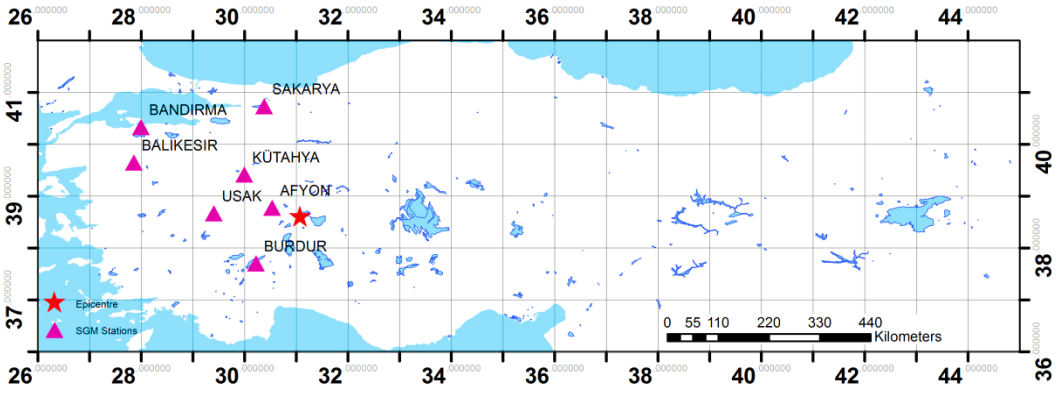

Figure 3.4: Location of strong ground motion stations that recorded 3 February 2002 Çay earthquake

Initially strong motion data is checked for baseline correction and filtered with forth-order Butterworth filters to band-pass the data within the frequency range of 0.25-25Hz. Further detailed information on strong ground motion stations used in this study are given in Table 1. Name and code of the station as in the database, coordinates and site classes based on NEHRP classifications are presented. More,i:over, peak horizontal ground accelerations and epicentral distances of the stations are also listed in the same Table.

Table 1: Detailed information on strong ground motion stations

Station	Code	Latitude (°N)	Longitude (°E)	Mean $V_{s_{30}}$ (m/s)	Site Class NEHRP	R_{epi} (km)	R_{rup} (km)	R_{jb} (km)	PGA (cm/s^2)	
									NS	EW
Afyon-Merkez	AFY	38.776	30.534	226	D	64.71	57.68	51.67	123.13	96.37
Burdur-Merkez	BRD-2	37.704	30.221	294	D	124.94	114.21	112.69	2.33	2.67
Uşak-Merkez	USK	38.671	29.404	285	D	157.48	146.69	144.43	7.64	5.69
Kütahya-Merkez	KUT	39.419	29.997	243	D	144.41	135.22	132.77	23.13	22.88

3.4 Model Parameters

In order to simulate the ground motions accurately, the most important step is to define the input model parameters properly. Definitely, the input seismological parameters derived from the local data are required for reliable models. In case the regional studies or data are not sufficient to derive these model parameters locally, generic parameters can be used in simulations with care such that these generic parameters are derived for similar seismotectonics or site classes elsewhere in the world. In this part of the study, the derivation and definition of model parameters for the region of interest are presented.

3.4.1 Source Parameters of 2002 Çay Earthquake

Since the near-field ground motion distribution is of concern in this study, finite-fault modeling of the ground motions is used as the main methodology. The required source parameters are as follows: dip and strike angles, length and width of the fault rupture plane, hypocentral depth, epicentral coordinates, slip distribution along the fault plane, stress drop, and pulsing area percentage. Among different models (Harvard, 2002; NEIC, 2002; EMSC, 2002; INGV, 2002; USGS, 2002; ETHZ, 2002; Taymaz et al., 2002; Aktug, 2009), the fault model of Aktug (2009) is employed in the simulations to minimize the misfit in the estimations. There is no available study about slip distribution along the fault plane for Çay earthquake, therefore random slip distribution is used in the EXSIM code which satisfies the moment magnitude of the event through conservation of the seismic moment.

Other than the faulting mechanism, the only other source parameters left are stress drop and pulsing area percentage as defined in Chapter 2. These parameters are determined after constraining all the other path and site parameters in order to minimize the misfit between observed and synthetic records.

3.4.2 Path Parameters of the Çay Earthquake

To define wave propagation in the Earth, there are three major parameters: geometric spreading, quality factor and duration model. For geometric spreading and duration, there are no studies available in the region of interest; partly because there is not sufficient data collected from past events. Thus, generic factors obtained from worldwide data are used for geometrical spreading and duration. For anelastic attenuation however, the study of Akinci et al. (2013) yields a regional quality factor which is employed in this study.

The geometric spreading factor can be represented as follows:

$$R^{-1} \qquad R \leq 30\ km \tag{2.1}$$

$$R^{-0.5} \qquad 30 < R \leq 1000\ km \tag{2.2}$$

This model states that seismic waves decrease in amplitude faster in near-field than in the intermediate- and far-field.

Distance-dependent duration model is adapted from Herrmann (1985) and given as:

$$T = T_0 + 0.05R_{hypo} \tag{2.3}$$

where T_0 is the source duration in seconds, R_{hypo} is the hypocentral distance in km. This model states that the duration of the seismogram increases during wave propagation from the hypocenter until the wavefront reaches the observation point.

The anelastic attenuation model is adapted from the study of Akinci et al. (2013) in which data from Western Anatolia is employed. The reason for selecting this model is the similarities in tectonics of the studied regions. Faulting mechanism of Çay earthquake is represented as normal with a minor slip component which is compatible to the tectonics of the region investigated in the study of Akinci et al. (2013). Similarly, properties of the crustal and near-field Earth media in both regions is as well comparable. The form of the quality factor is given as follows:

$$Q_f = 180f^{0.55} \tag{2.4}$$

3.4.3 Site Effects at the Stations that Recorded the 2002 Çay Earthquake

The final set of input parameters is the site model parameters as described in Chapter 2. The true reflection of the site response is extremely important in simulations since the frequency-dependent amplification factors directly affect the amplitudes of deterministic spectrum in the stochastic model.

Site response is composed of two major factors, amplification and diminution. As described in Chapter 2 in detail, two different approaches exist to compute amplifications; empirical and theoretical method. In order to get the most accurate estimation, in this thesis both methods are studied and compared to each other.

In H/V method, for each of the stations the ratio of Horizontal Fourier Amplitude Spectrum to Vertical Fourier Amplitude Spectrum of the S-wave portion of each record is computed. The average H/V values from 30 records per each station yield the empirical amplification spectrum of that site. Mean empirical amplification factors for each site can be seen in Figure 3.5.

As explained in Chapter 2, vertical component of the ground motions is less exposed to amplification through soil media than the horizontal component. Thus, when the ratio of horizontal to vertical FAS is used as the amplification spectrum, the near surface effect of the vertical ground motion is not taken into account. As a result, if the empirical amplification factor is used in the analysis, vertical kappa factor should be considered (Motazedian, 2006) not the horizontal one.

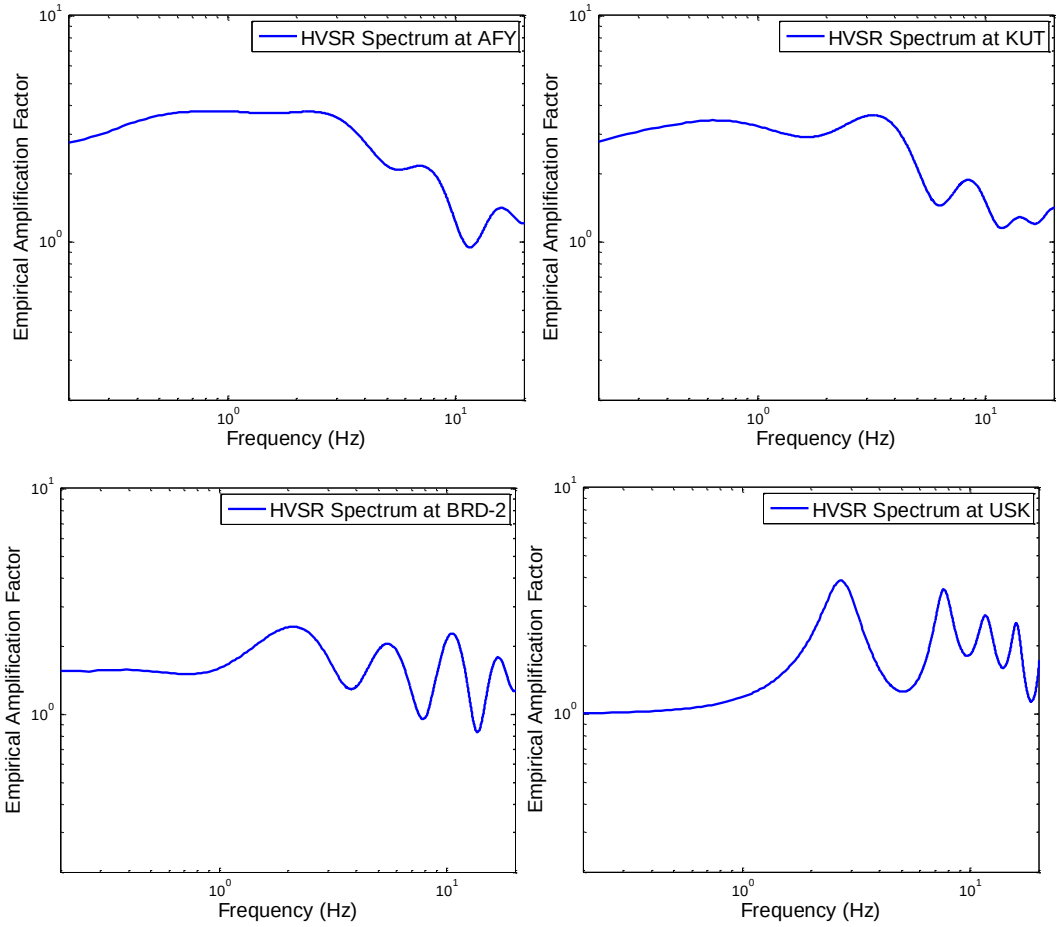

Figure 3.5: Mean empirical amplification factors at ground motion stations

Since the velocity profile of the sites down to 30 meters is known in this study, theoretical amplification factors could be calculated. Even though the velocity profile of each site is available, it might involve uncertainties due to difficulties in measuring velocity values of deeper soil layers. Therefore, by modifying the given profile using SPT counts, the best geotechnical estimations are attempted for each site separately. The calibrated velocity profile of each station is given in Figure 3.6. The analysis is performed using equivalent linear approach in DeepSoil Software. Further details on the soil layers of the stations can be found in detailed borehole logs at the online DAPHNE database.

Site-response analyses require ground motion records as input at the bedrock level; and yield the surface acceleration and the transfer function as outputs. In this study, the Sakarya record from the 17 August 1999 Kocaeli event (measured on stiff soil) is used.

Calibrated shear wave velocity profile of each site are displayed in Figure 3.6.

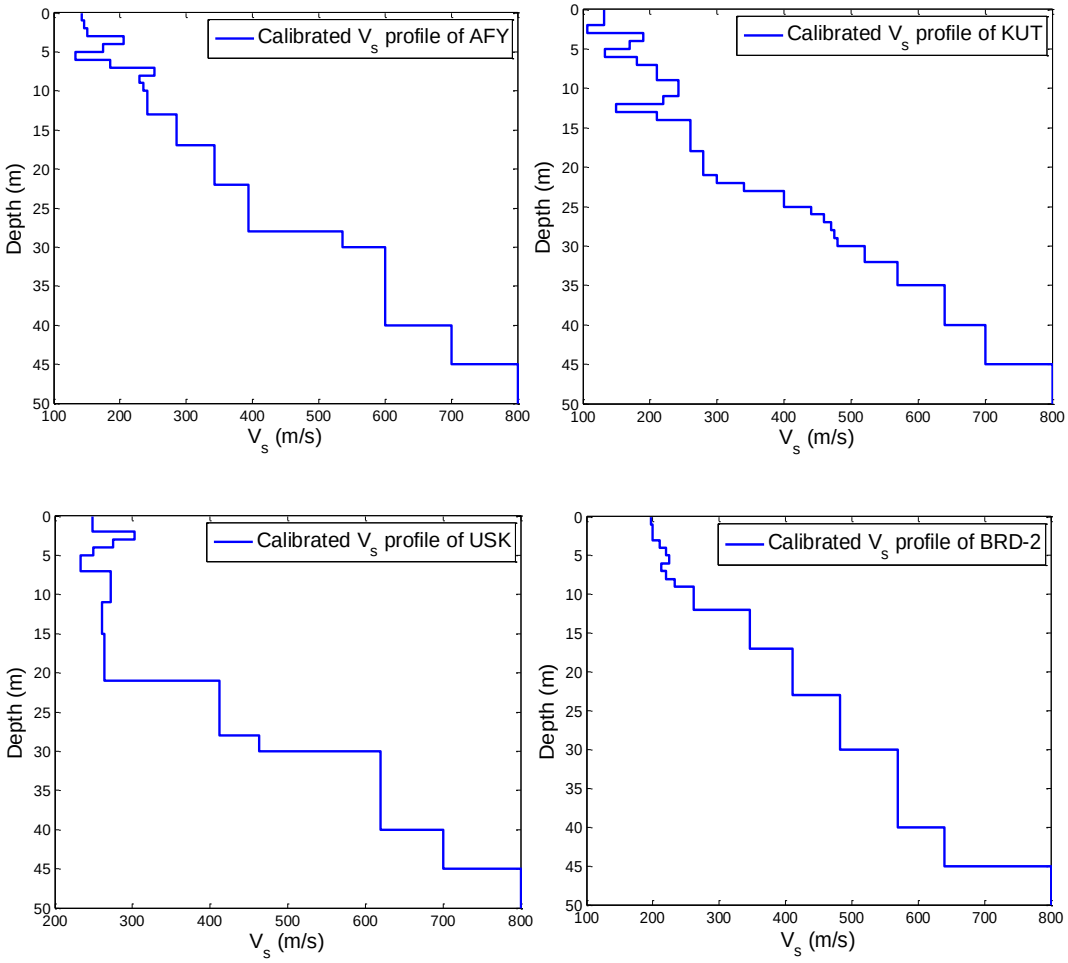

Figure 3.6: Calibrated shear wave velocity profiles of sites

Theoretical amplification factors (transfer functions) of each site are displayed in Figure 3.7.

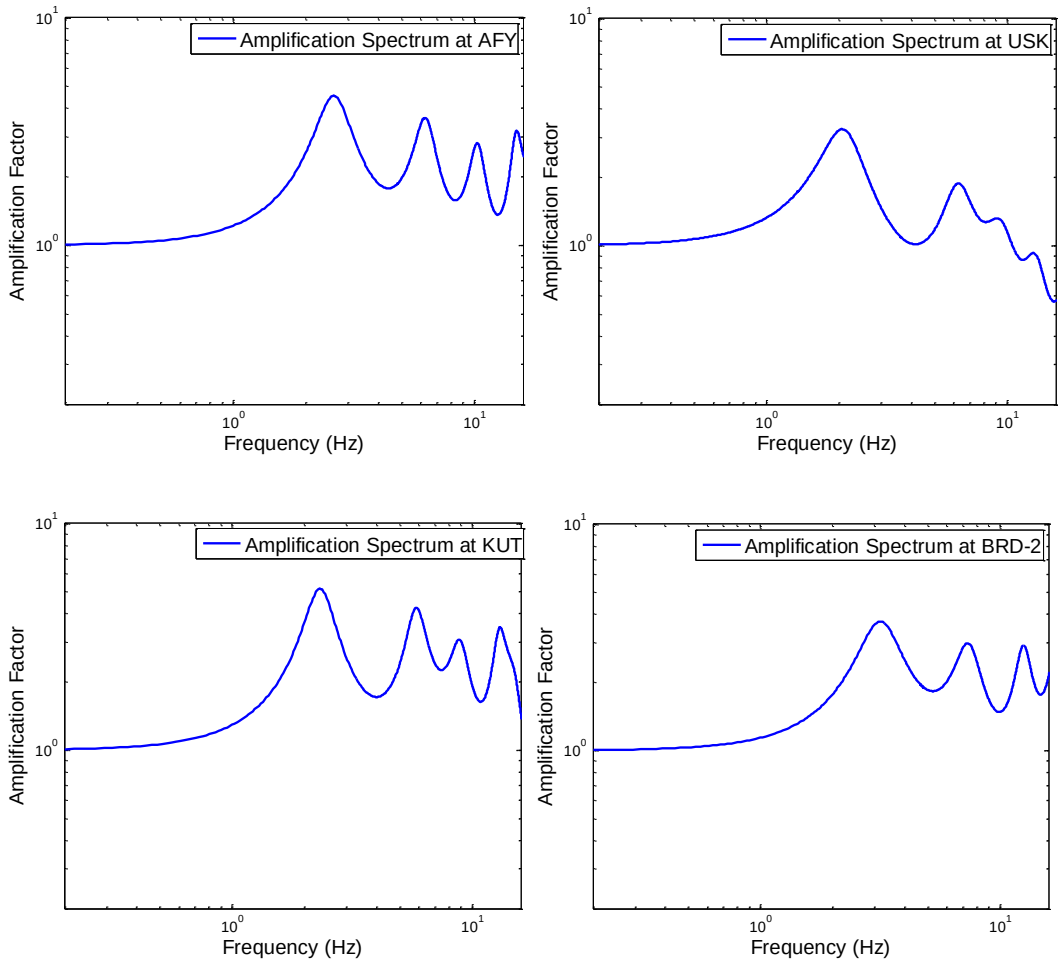

Figure 3.7: Theoretical amplification factors of ground motion stations

The empirical and theoretical amplifications are compared in Figure 3.8. At Uşak and Burdur stations, two approaches are observed to be consistent. However, in Afyon and Kütahya, the empirical functions do not yield any dominant peaks or consistent amplitudes. This difference is attributed to the insufficient quality of the records at those stations yielding unreliable H/V ratios.

Since the number of ground motions recorded at each site and the quality of some records are insufficient; the estimations obtained by empirical methods are in general less reliable. Therefore, in this study, theoretical amplification factors are employed for the sake of employing accurate site effects in the simulations.

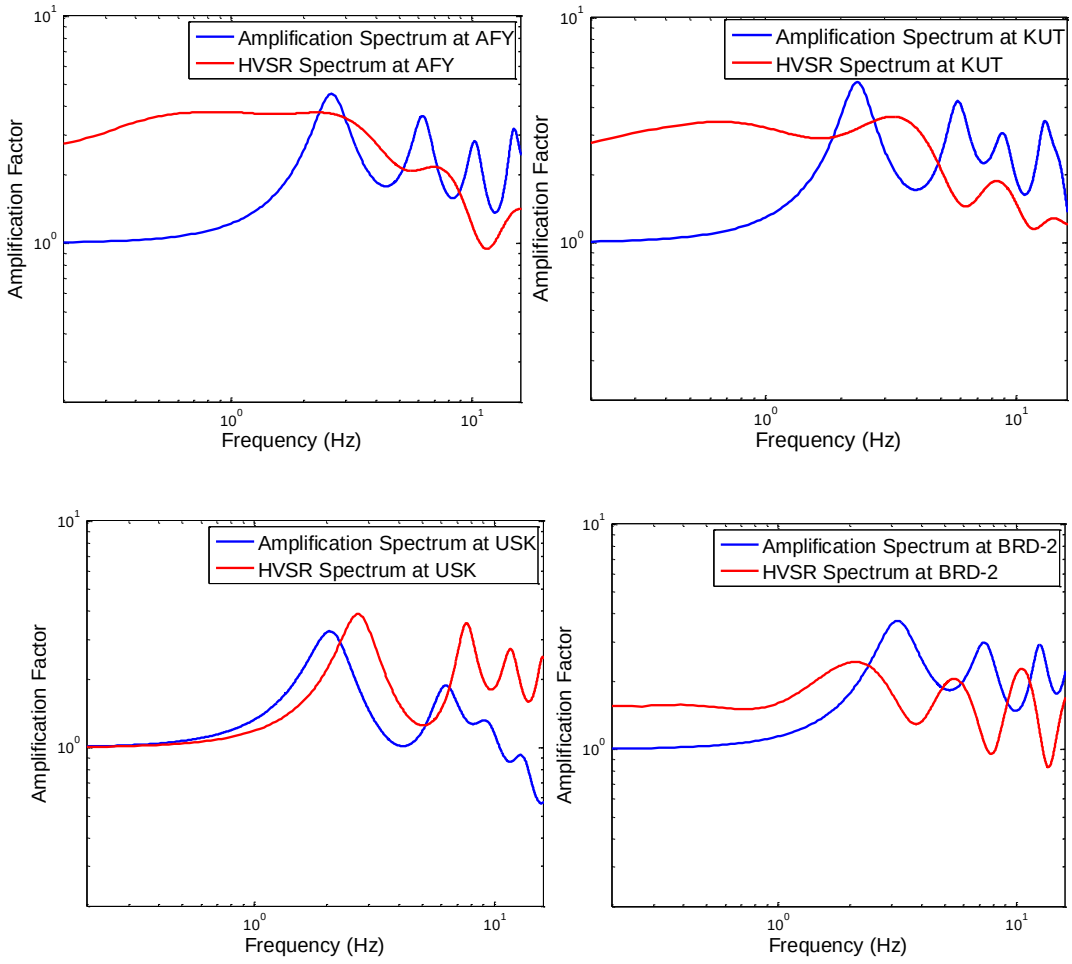

Figure 3.8: Comparisons of empirical and theoretical amplification of ground motion stations

The second site parameter is kappa (κ) factor, which models the linear decay in higher frequencies of Fourier Amplitude Spectrum of S-wave portion of the acceleration records in semi-logarithmic space. Kappa value of each record is estimated from the smoothed Fourier Amplitude Spectrum of that record (Anderson and Hough, 1984). While estimating the kappa factor of a site, a non-automatic technique is used since the end points of spectral decay vary for each record. (Douglas et.al, 2009; Askan et al., 2014).

After computing the kappa factors from 30 records per station, the kappa values are plotted against epicentral distances of each record. In order to eliminate the anelastic attenuation effects from the kappa factor, zero-distance, κ_0 value is calculated which is simply the y-intercept of a linear approximation to the data. In other words, a kappa model is fit for each station in the form of $\kappa = \kappa_0 + p * R_{epi}$ where p is a region-dependent slope value. κ_0 is the near-surface attenuation value where there is no attenuation contribution from the path effects. Kappa factors at each site are shown in Figure 3.9-Figure 3.12.

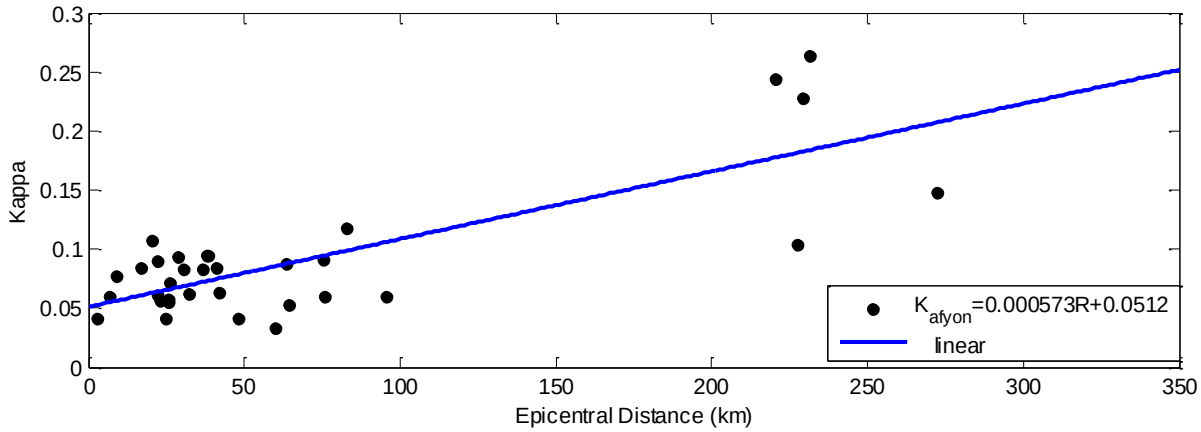

Figure 3.9: Kappa model at AFYON station

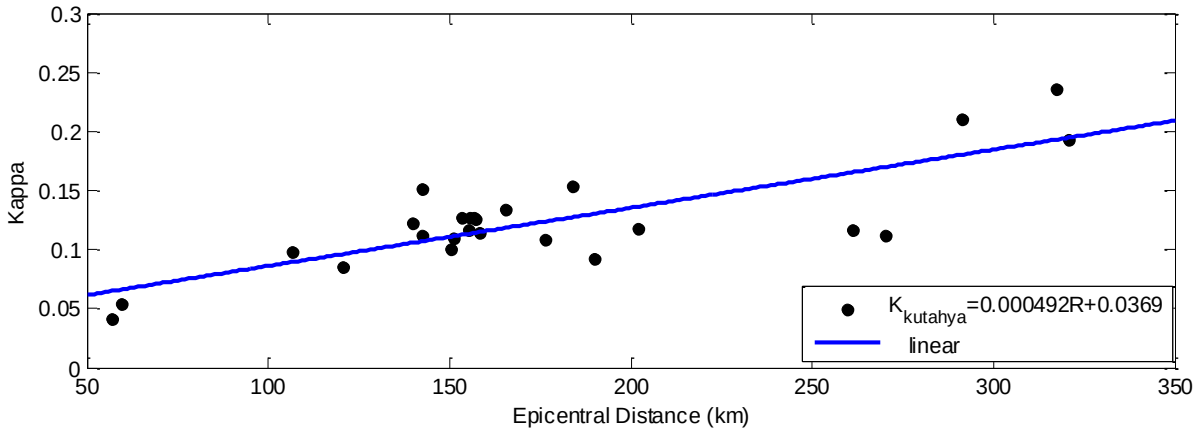

Figure 3.10: Kappa model at KÜTAHYA station

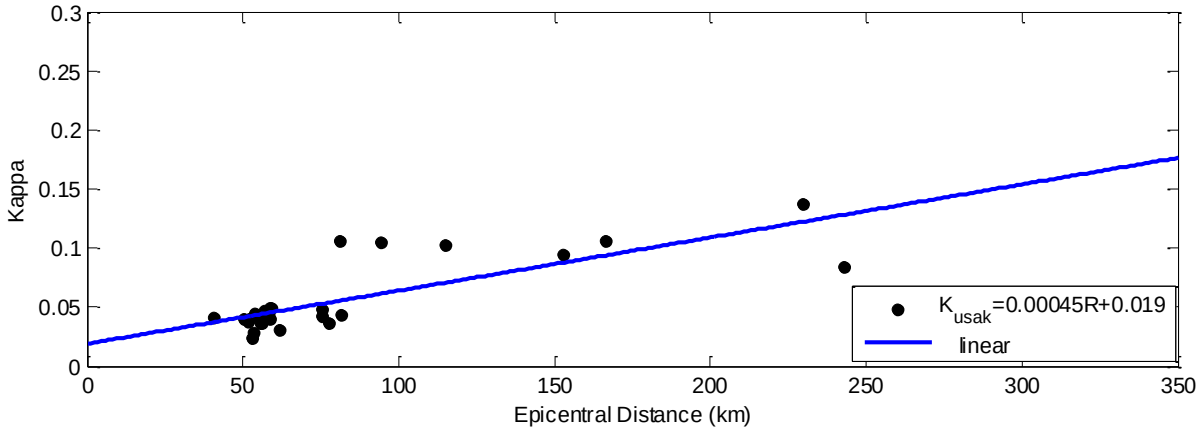

Figure 3.11: Kappa model at UŞAK station

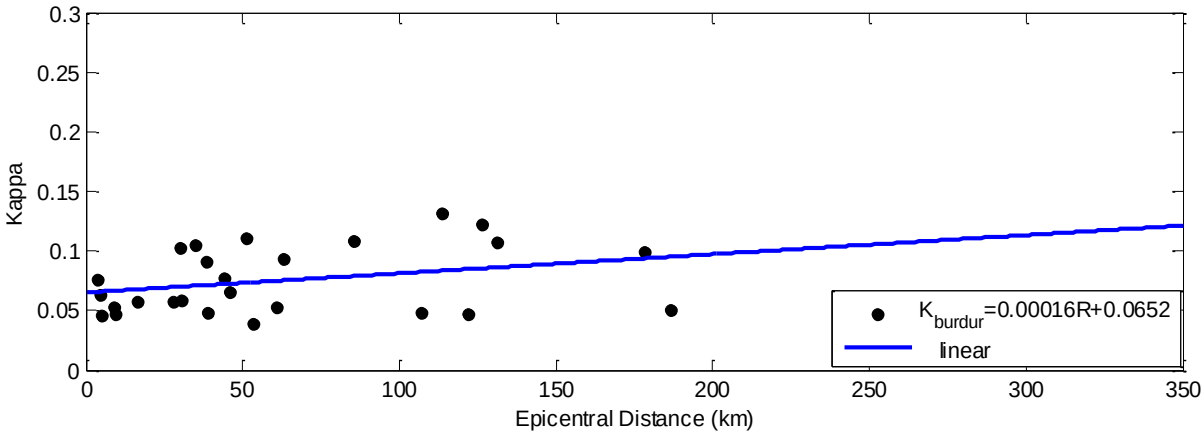

Figure 3.12: Kappa model at BURDUR station

3.4.4 Optimal Model Parameters Used in the Simulations

The final two parameters of simulations are the stress drop and pulsing area percentage. Determining the value of stress drop is not a straightforward procedure since it is directly related to the energy that the fault released when the earthquake occurred.

To decide the optimal values of these parameters that are not fixed, a frequency-dependent misfit criterion is employed in the form of $E(f) = \log(\frac{A_i(f)_{\text{observed}}}{A_i(f)_{\text{synthetic}}})$ at all stations.

After calculating error between observed and simulated fourier spectra, a sensitivity index (SI) is detemined by using the following formula at each station for corresponding stress drop values (σ):

$$SI = \frac{1}{n_{freq}} \sum log\left(\left|\frac{A_i(f)_{observed}}{A_i(f)_{synthetic}}\right|\right)$$

Table 2: Error Calculation with different stress drop values at each site

STATION	ERROR σ=30 bar	ERROR σ=45 bar	ERROR σ=60 bar	ERROR σ=75 bar
Afyon-Merkez	0.00031	0.00019	0.00011	0.00005
Burdur-Merkez	0.00021	0.00015	0.00011	0.00007
Uşak-Merkez	0.00058	0.00052	0.00049	0.00046
Kütahya-Merkez	0.00059	0.00053	0.00049	0.00046

By considering all of the stations, stress drop is selected to be 45 bars in the simulations to minimize the error in the approximations and to control higher frequencies of the spectra. This stress drop value of 45 bars is also similar to the value obtained from the study of Mohammadioun and Serva (2001) which supplies theoretical and empirical relations between source dimensions and stress drop. Those relationships yield a stress drop value around 45 bars given the fault dimensions of the Çay earthquake.

After fixing the spectral amplitudes of higher frequencies of the Fourier Amplitude Spectra with the previous parameters, the lower frequency portion of the FAS is checked by adapting different values of pulsing area percentage iteratively (Motazedian and Atkinson, 2005).

Finally, 50% pulsing area percentage and 45 bar stress drop values are used in the simulation for all sites since the source properties do not vary from site to site.

In Table 3, the optimal source, site and path parameters used in the simulations are displayed.

Table 3: Model parameters used in the simulation of Çay earthquake

Parameter	Value
Moment Magnitude	6.6
Hypocenter Location	38°36'32.4"N 31°46'36"E
Hypocenter Depth	5 km
Fault Orientation	Strike:271°, Dip: 43°
Fault Dimensions	33 x 12 km
Subfault Dimension	3 x 2 km
Windowing Function	Saragoni-Hart
Attenuation Model	$Q(f) = 180f^{0.5}$
Duration Model	$T = T_0 + 0.05R_{hypo}$
Geometric Spreading	R^{-1} $R \leq 30\ km$ $R^{-0.5}$ $30 < R \leq 1000\ km$
Crustal Shear Wave Velocity	3700 m/s
Rupture Velocity	3000 m/s
Crustal Density	2800 kg/m^3
Stress Drop	45 bar
Pulsing Area Percentage	50%
Amplification Factor	Local Theoretical Amplification of Each Site

3.5 Simulation Results: Comparison of Observed and Simulated Waveforms at the Stations

Using the parameters specified previously in Table 2, strong ground motion simulation is performed for 3 February 2002 Çay earthquake.

Since the motion is recorded only by four stations within the epicentral distance of 200 km, the method is applied for these sites mostly for studying near-field effects. For comparison purposes, Fourier Amplitude Spectra and acceleration time histories are computed. The comparison of FAS and time histories for synthetic ground motions against the observed records are shown in Figure 3.13-Figure 3.20. In these figures, red curve represents NS component of the ground motion, black curve stands for EW component and blue curve is the simulated motion. The comparisons are made in terms of amplitudes, duration and frequency content.

Simulations yield mostly conservative peak ground acceleration values at stations BRD-2, KUT and USK. In particular, at BRD-2 the amplitudes in time-domain are significantly overestimated. On the other hand, simulated PGA and the overall amplitudes at AFY station match the corresponding real values closely. The duration of the synthetic motions for AFY, USK and BRD-2 stations match with recorded motions while for the KUT station, the simulated total duration is underestimated when compared to the real ground motion. However, for all cases shear-wave durations are compatible. The difference in the total duration is basically due to the fact that the stochastic model considers only the S-wave portion of the accelerogram while surface waves increase the duration of real records.

When the FAS are considered for the frequency content and spectral amplitudes, at all of the sites other than BRD-2, a sufficient match is observed in the high frequency range. This observation points to the careful selection of the input parameters. However, at BRD-2, despite the close match at higher frequencies, the observed

spectrum is simply flat for frequencies less than 4 Hz which is unrealistic considering the theoretical spectrum shape. At that station, both time domain and frequency domain data seems unphysical which might actually indicate failure of the instrument.

The FAS comparison at AFY yields a very close match at all frequency ranges consistent with the time-domain comparisons. Since this is the closest station from the source, the match at this station indicates an efficient near-field simulation. Considering FAS at KUT, other than the frequency range of 0.3-0.6 Hz, the observed spectrum is simulated effectively. When the USK station is examined, a slight overestimation at higher frequencies is observed along with a noticeable overestimation at low frequencies. The mismatch of FAS might mostly indicate an issue in site effects since the source and path parameters are validated at AFY station in both time and frequency domains.

It must be noted that all stations other than AFY are located in the backward directivity direction. AFY station does not show any distinct features and is simulated successfully. However, the lower amplitudes and longer durations at USK, KUT and BRD-2 stations could be due to backward directivity conditions. Stochastic source models do not fully consider such source complexities which might explain the low-frequency mismatch in FAS.

Lastly, none of the records obtained from the mainshock is composed of completely free field ground motion since the accelerograms are located in the buildings. Thus, possible contribution of building response in the records could interfere with the comparison of free-field simulations with the data.

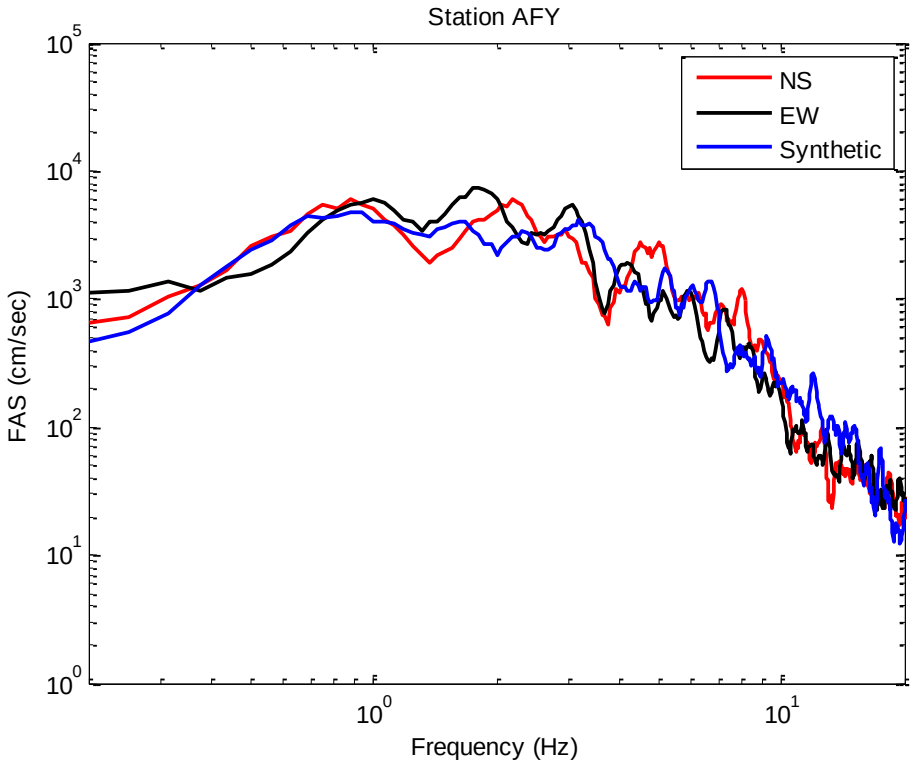

Figure 3.13: Comparison of synthetic and observed FAS at AFYON

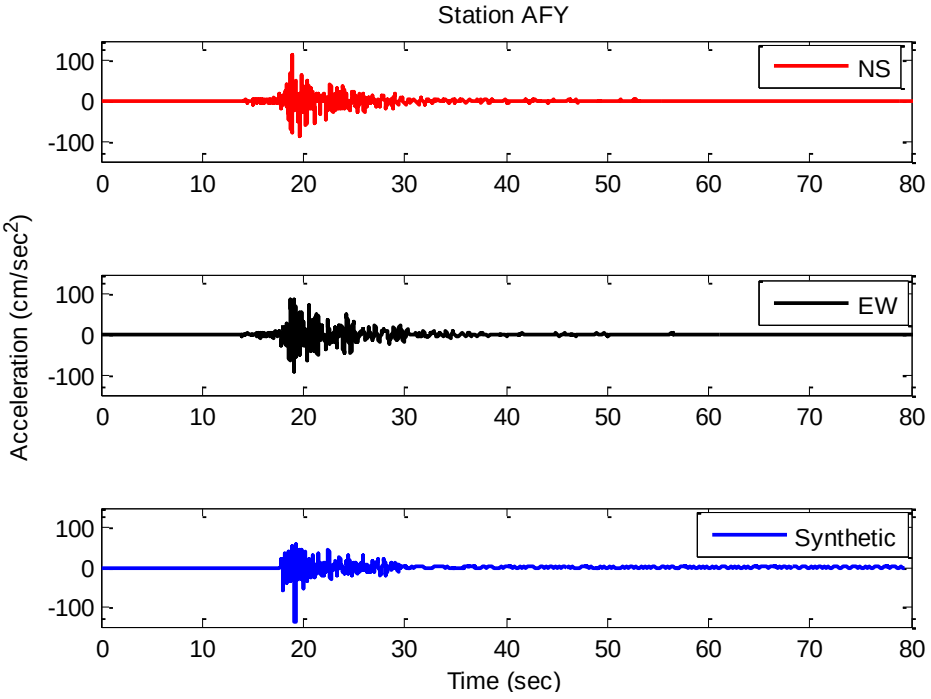

Figure 3.14: Comparison of synthetic and observed time histories at AFYON

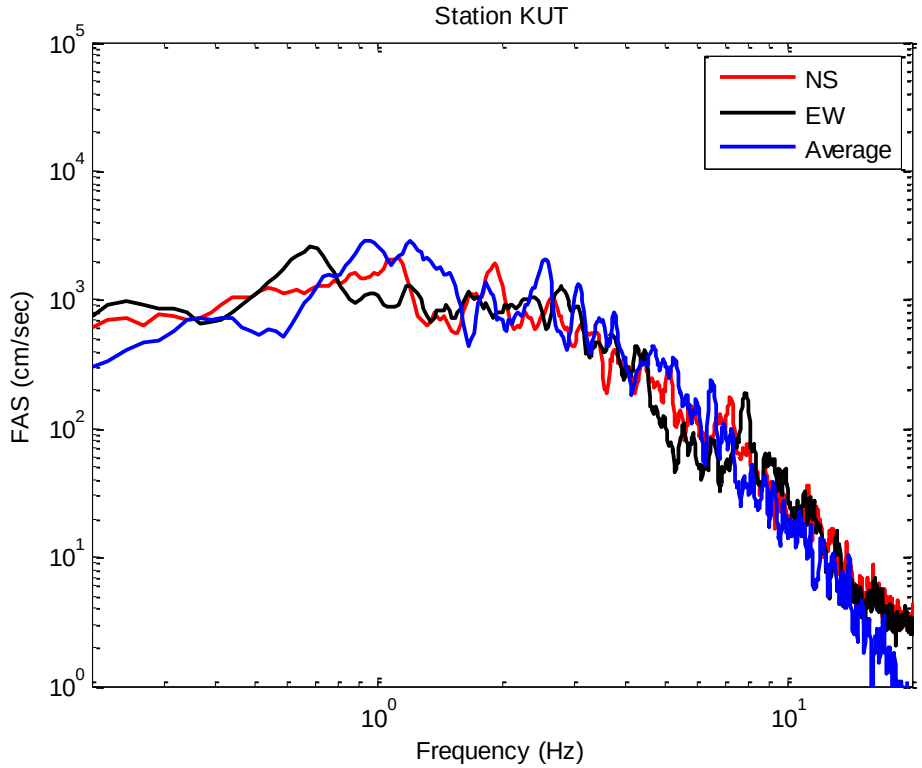

Figure 3.15: Comparison of synthetic and observed FAS at KÜTAHYA

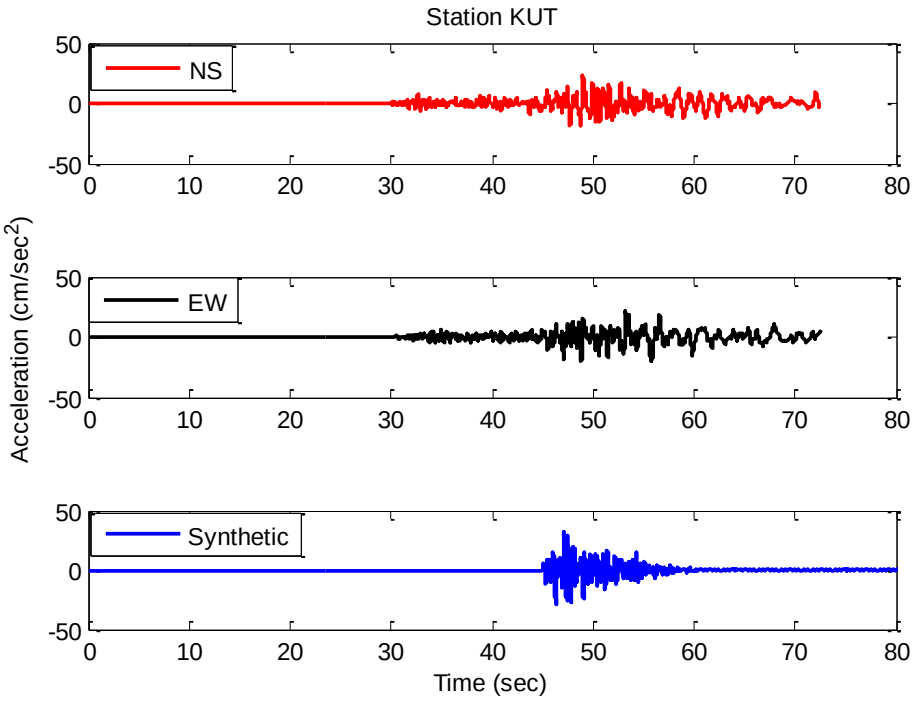

Figure 3.16: Comparison of synthetic and observed time histories at KÜTAHYA

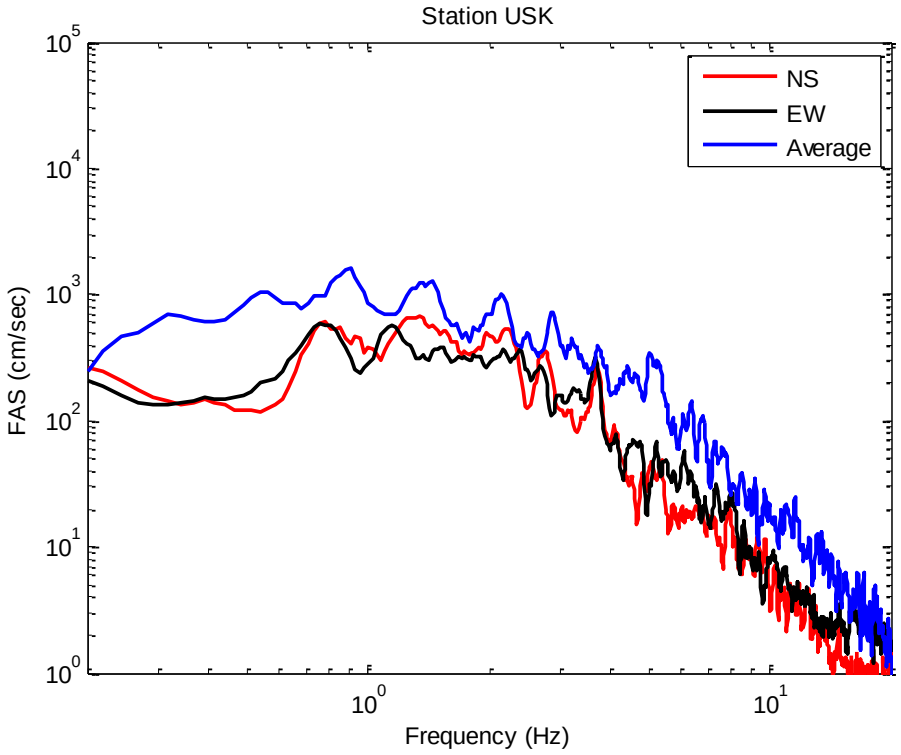

Figure 3.17: Comparison of synthetic and observed FAS at UŞAK

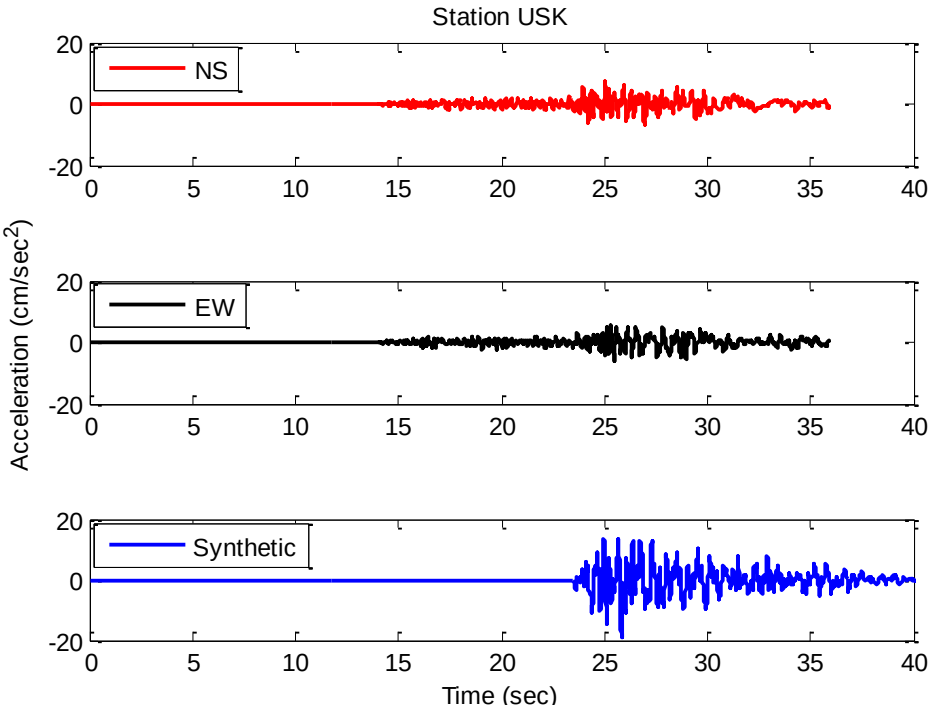

Figure 3.18: Comparison of synthetic and observed time histories at UŞAK

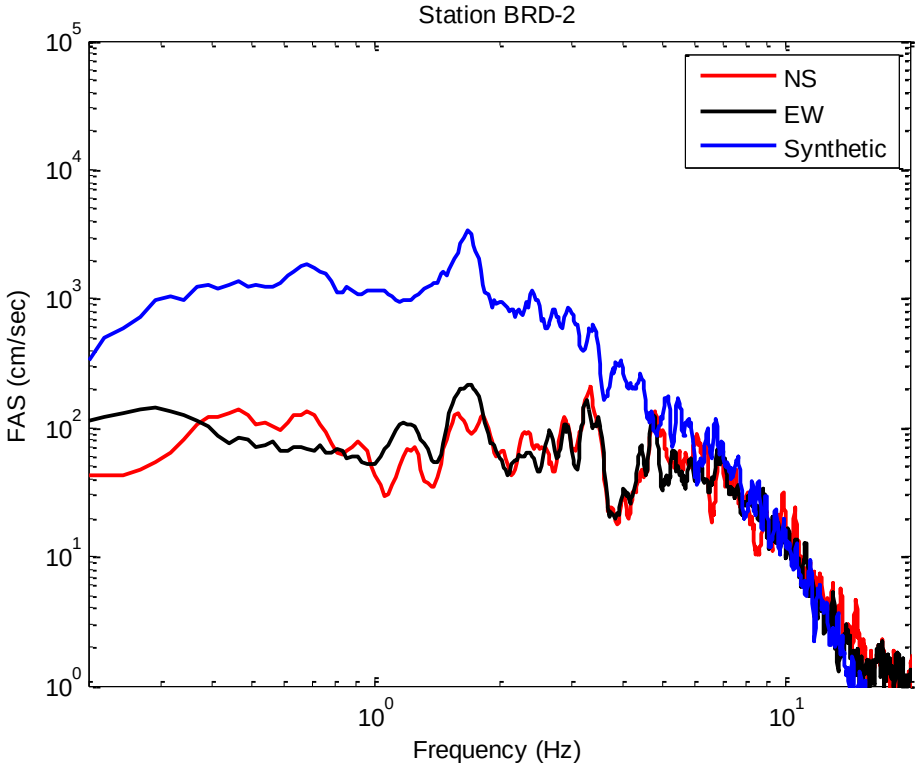

Figure 3.19: Comparison of synthetic and observed FAS at BURDUR

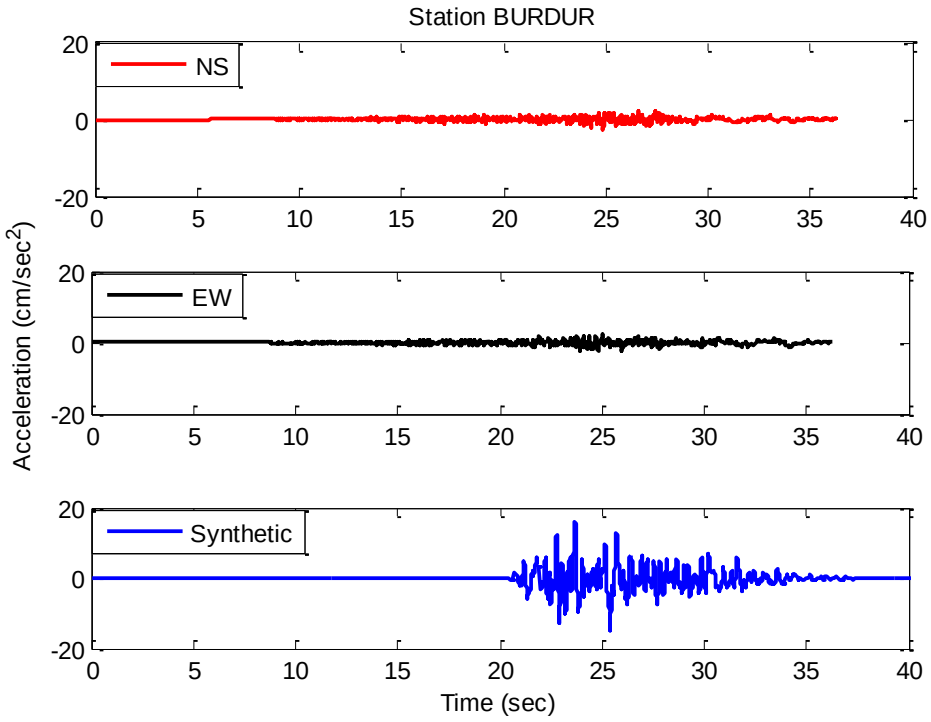

Figure 3.20: Comparison of synthetic and observed time histories at BURDUR

Table 4: Comparison of Observed and Simulated PGA at each station

Station	Code	R_{jb} (km)	PGA-observed (g)		PGA-simulated (g)
			(NS)	(EW)	
Afyon-Merkez	AFY	51.67	0.126	0.098	0.143
Burdur-Merkez	BRD-2	112.69	0.002	0.003	0.017
Uşak-Merkez	USK	144.43	0.008	0.006	0.019
Kütahya-Merkez	KUT	132.77	0.024	0.023	0.033

3.6 Blind Simulations around the Epicentral Area

To further validate the results, blind simulations are performed at 625 nodes where there are no records (dummy stations) around the epicentral area within Afyon province. The nodes are specified by a rectangular grid distribution pattern. This blind simulation exercise serves two major purposes: one is to compare the attenuation of the synthetics with distance against existing ground motion prediction equations; second is to validate the spatial distribution of the simulated intensity with the corresponding observed values.

3.6.1 Comparison of Synthetics with Ground Motion Prediction Equations

Comparisons of the attenuation of the simulated records against three GMPEs are presented herein. The blind simulation is performed for Afyon province where 625 dummy stations are placed.

The source and path effects are simulated with the values given in Table 2. On the other hand, an assumption is made in terms of site effects: At all dummy stations the theoretical amplification factors developed for Afyon and κ_0 value computed at Afyon site is used. In other words, uniform site conditions are assumed in Afyon province.

For space reasons, it is not possible to display the full time histories simulated at 625 stations. However, from the full time histories, spectral accelerations with 5% damping ratio at T=0.3, 1.0 and 2.0 sec are calculated at these dummy stations. The spatial distributions of simulated PGA and SA at the mentioned periods are shown in

Figure **3.21**- Figure 3.24. A maximum PGA of 0.44g is observed around Çay province closest to the epicenter while at the same location SA (0.3 s), SA (1s) and SA (2s) reach 0.93g, 0.34g, 0.11g respectively. The anticipated (simulated) ground motions during the event confirm the damage levels observed in the epicentral area. Further discussions are provided in 3.6.2.

Next, the attenuation of synthetics are compared to GMPEs by Chiou and Youngs (2008), Abrahamson and Silva (2008) developed within the scope of Next Generation of Attenuation (NGA) Relations Project. In addition, a local study by Akkar et.al. (2013) derived with data from Europe and Middle East is also used. For all the dummy stations the $V_{S_{30}}$ value of 226 m/s (as measured in AFYON station) is employed in the GMPEs. Figure 3.25-Figure 3.28 display these comparisons. The attenuation of the synthetic PGA values and the spectral accelerations at all selected periods remain within the range of at most one standard deviation of the GMPEs. The results show that the GMPE by Chiou and Youngs (2008) gives the closest attenuation characteristics to that of simulated records. The local GMPE did not yield the closest form to the attenuation of simulated data most probably because the strong motion data of Turkey which is used in this local GMPE comes from the events on North Anatolian Fault zone, not from the region of interest due to the scarcity of data in Central Anatolia.

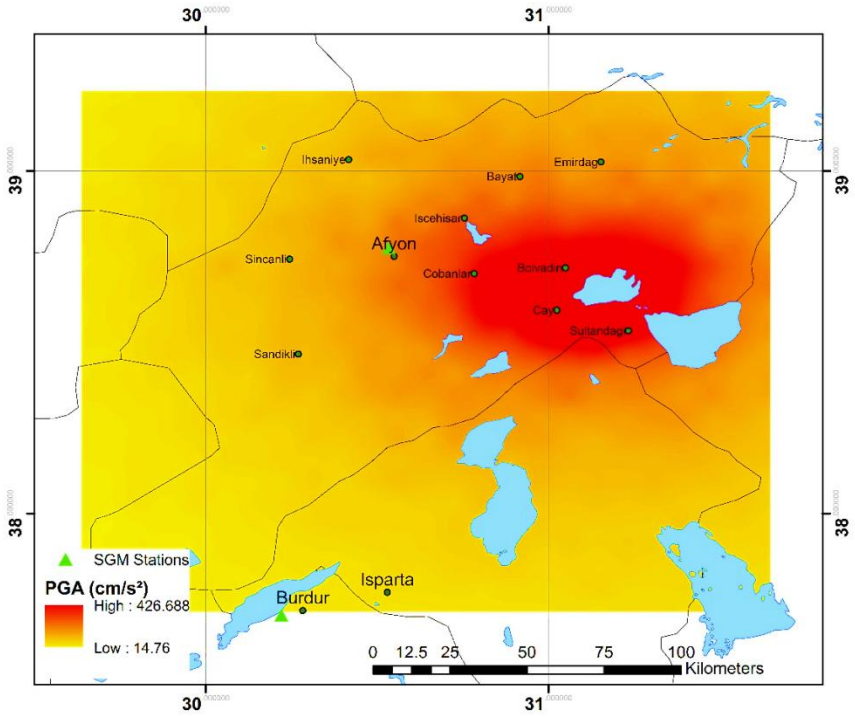

Figure 3.21: Spatial distribution of PGA in AFYON region

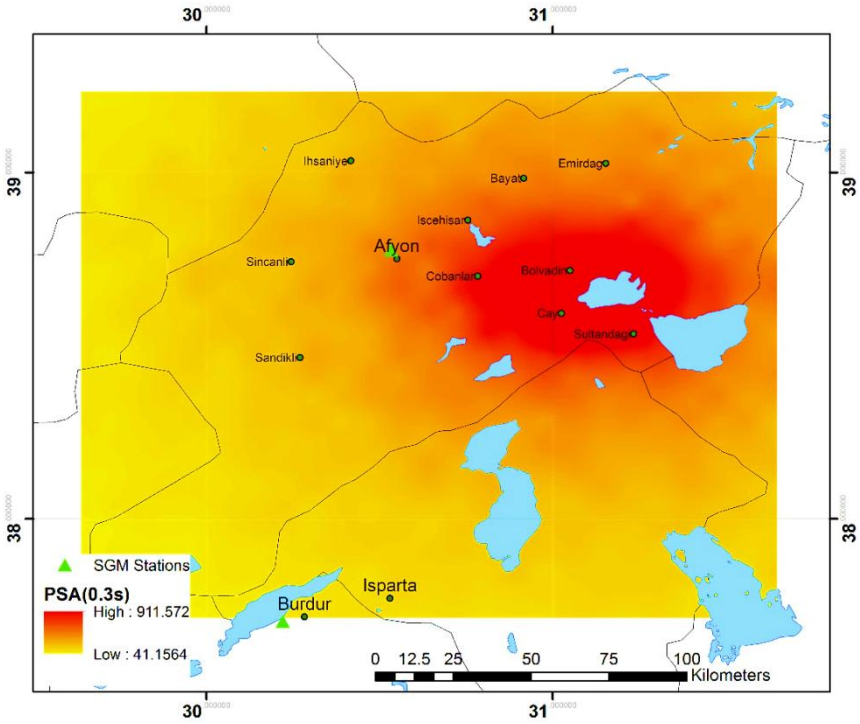

Figure 3.22: Spatial distribution of Spectral Acceleration at T=0.3sec

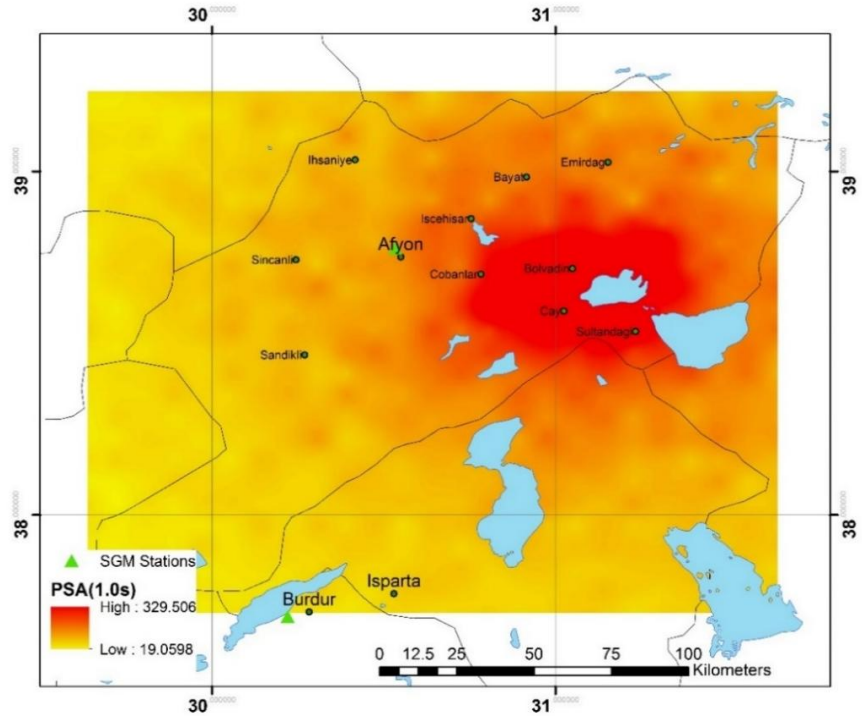

Figure 3.23: Spatial distribution of Spectral Acceleration at T=1.0sec

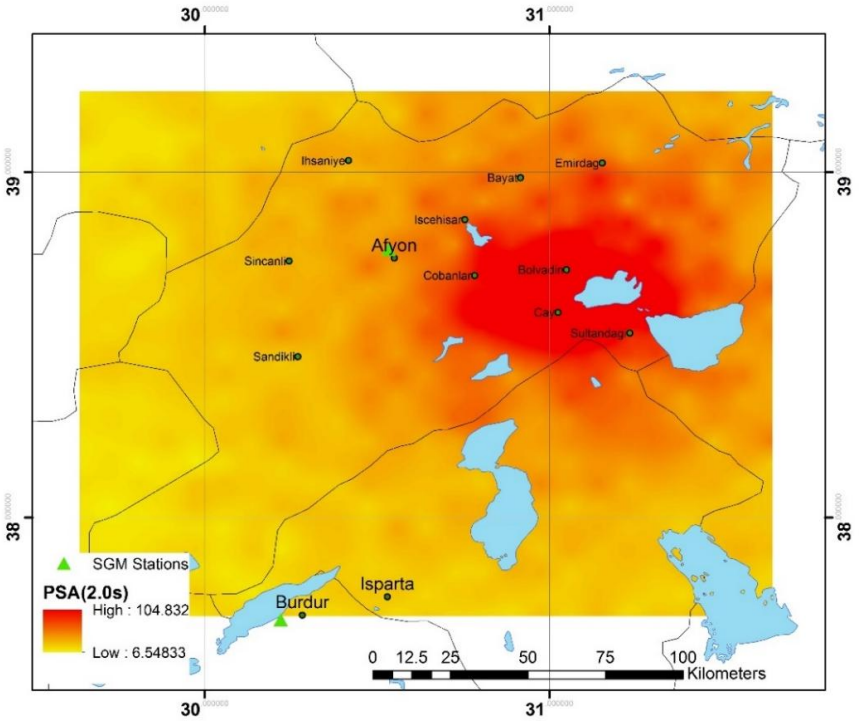

Figure 3.24: Spatial distribution of Spectral Acceleration at T=2 sec

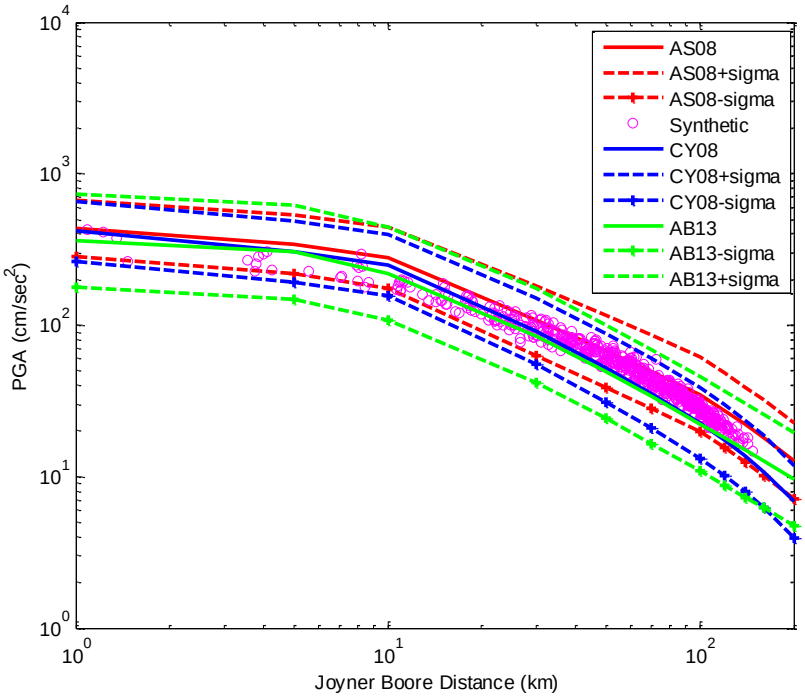

Figure 3.25: Comparison of GMPEs with the attenuation of synthetics in terms of PGA

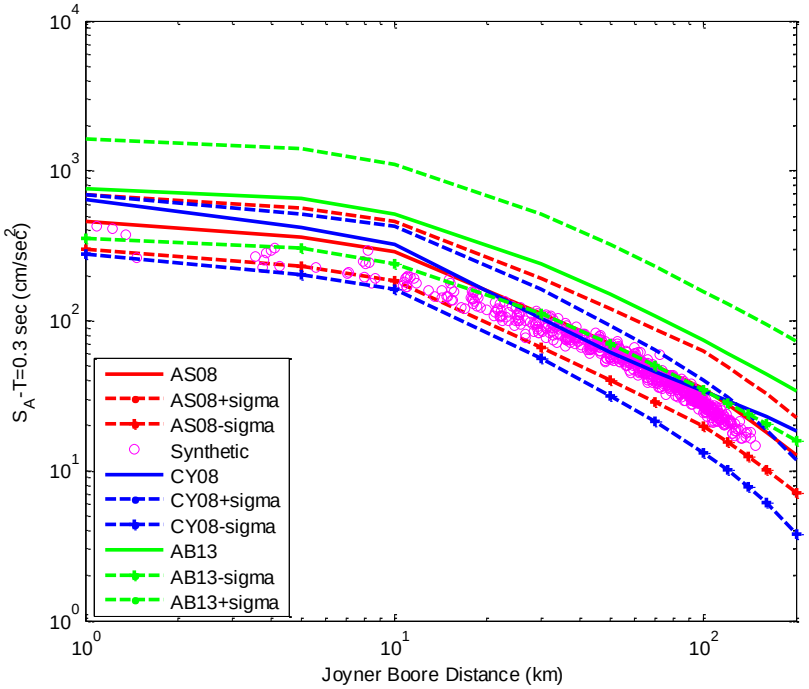

Figure 3.26: Comparison of GMPEs with the attenuation of synthetics in terms of SA at T=0.3 sec

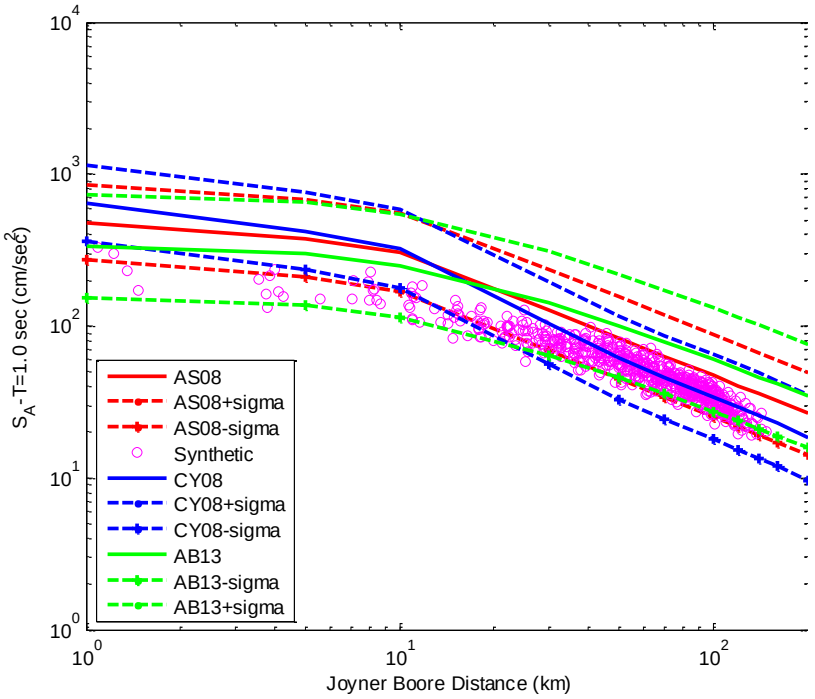

Figure 3.27: Comparison of GMPEs with the attenuation of synthetics in terms of SA at T=1 sec

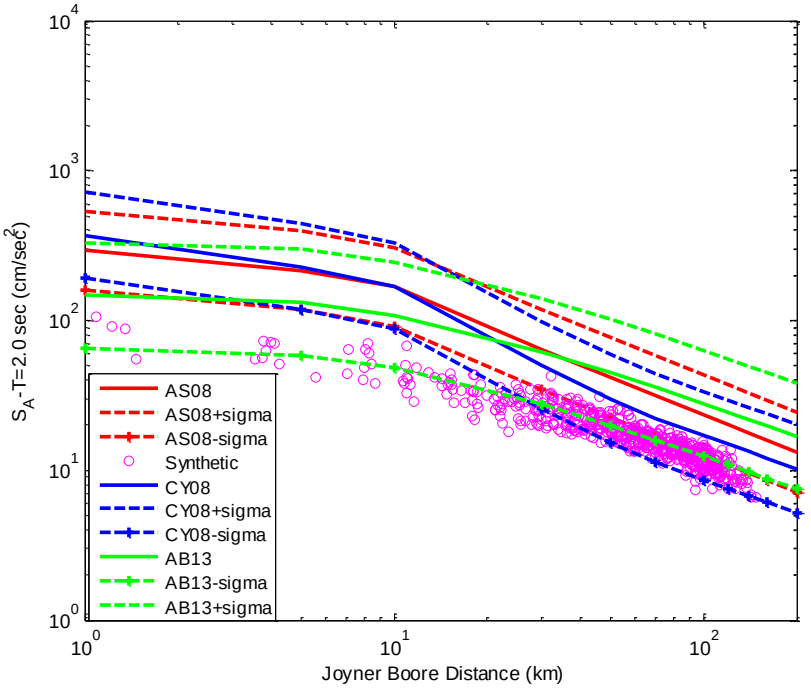

Figure 3.28: Comparison of GMPEs with the attenuation of synthetics in terms of SA at T=2.0 sec

3.6.2 Comparison of the Observed Intensity and Damage Distribution against Simulated Intensity Distributions

Recorded peak ground motion parameters such as PGA, PGV, and SA identify the severity of ground shaking during earthquakes in quantitative measures. However, a qualitative measure such as felt intensity can also be useful for rapid assessment and post-disaster management efforts. Seismic intensity values are decided based on human responses to ground shaking and observed damage in the nearby structures. Until recently, intensity measures such as Modified Mercalli Intensity (MMI) or Medvedev–Sponheuer–Karnik (MSK) scales had lost the original attention they had received due their subjectivity. However, recently the digital intensity maps prepared within the aftermath of large earthquakes gained importance since these intensity maps indicate the meizoseismal area affected from the event and provide guidance for the rapid assessment of shaking intensity and (indirectly) the physical damage (Bilal and Askan, 2014). Thus, efforts on correlating recorded ground motion parameters (PGA, PGV or SA) to felt intensity measures worldwide are continuously increasing (e.g.: Wald et al., 1999; Faenza and Michelini, 2010).

Similarly, a recent study by Bilal and Askan (2014) proposed empirical correlations between MMI- PGA/PGV/SA for Turkish earthquakes. The authors found that for reinforced concrete structures MMI-PGV relationship performs better; while for rigid masonry structures MMI-PGA relationship is more suitable. These conclusions confirm the following observations: PGA correlates better with damage for stiff wall-bearing masonry buildings, whereas PGV is used as the main ground motion intensity parameter for relatively more flexible reinforced concrete buildings (Erberik, 2008a, b).

In this study, a felt-intensity map of Çay earthquake is prepared for Afyon province by using the synthetic ground motion distribution at the 625 nodes explained previously. Since most of the damage occurred in multistory reinforced concrete

buildings in Çay Town (Kocyigit et. al., 2002; Gulkan et al., 2002) the MMI-PGV relationship is chosen from Bilal and Askan (2014):

$$MMI = 2.673 + 4.340 * \log(PGV)$$

Thus, the simulated PGV values are converted to MMI values at all nodes. The spatial distribution of this synthetic MMI values are then compared to the observed intensity map of the Çay earthquake prepared in the field (Kocyigit et. al., 2002) in Figure 3.29a.

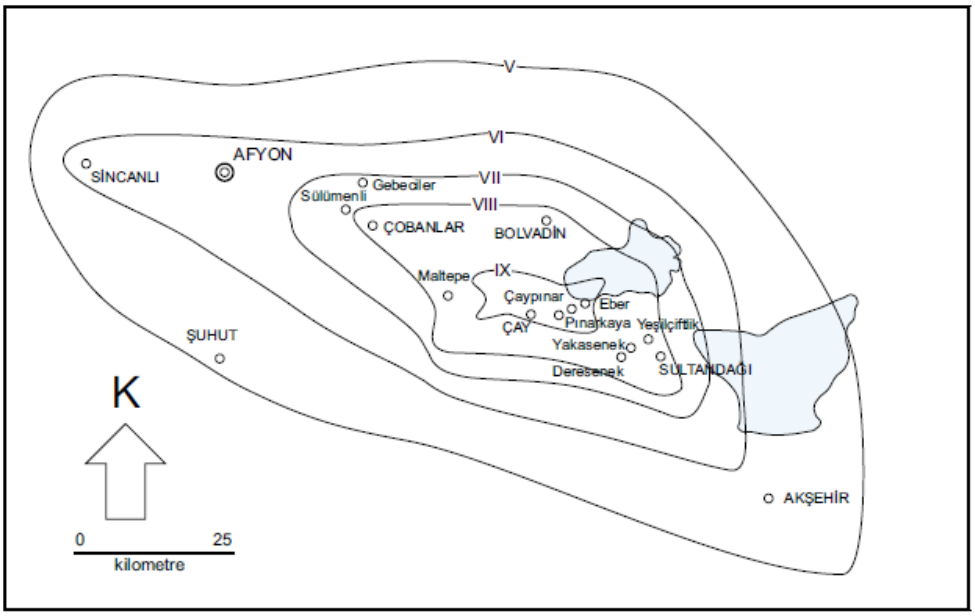

Figure 3.29a: Observed intensity map of Çay earthquake

(adapted from Kocyigit, 2002)

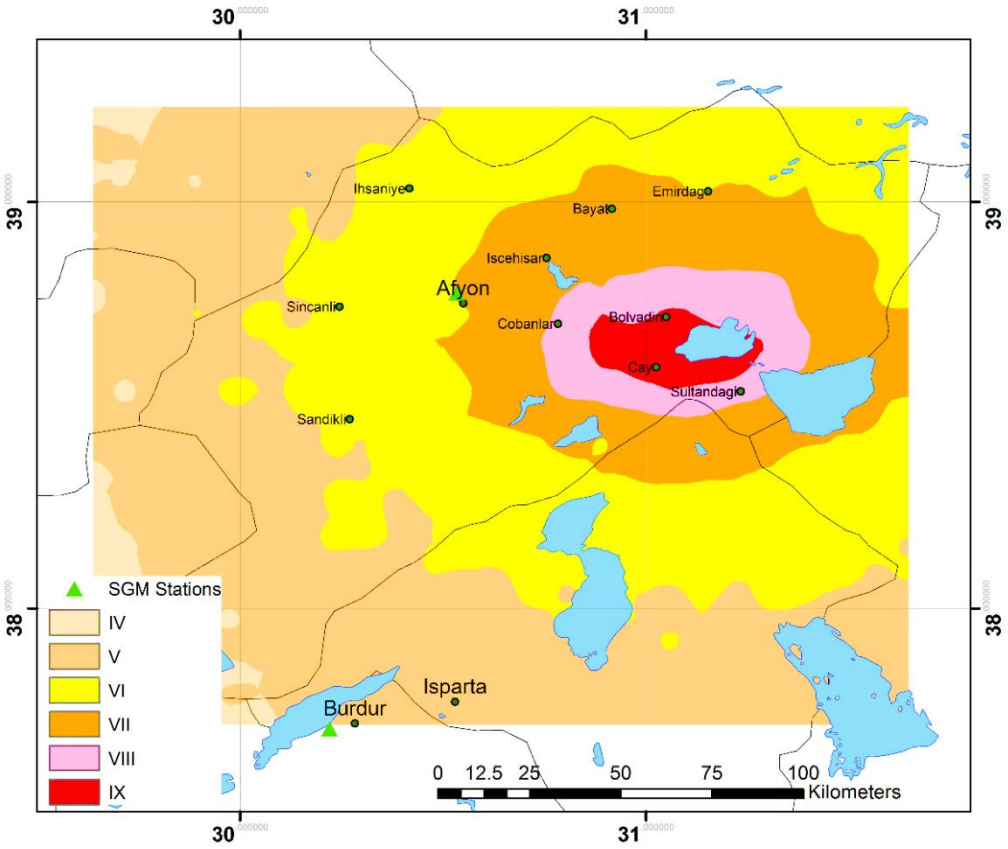

Figure 3.29b: Simulated intensity map of Çay earthquake

It is observed that the synthetic and actual intensity distribution is almost the same for most of the towns in Afyon province. The comparison of the intensity values for the towns specified in Kocyigit's study are shown in Table 5.

Table 5: Comparison of the Observed Intensity against Simulated Intensity for Afyon Province

Town	Observed Intensity	Simulated Intensity
Afyon (M)	6	6
Çobanlar	8	8
Sultandağı	8	8
Bolvadin	8	9
Çay	9	9
Sincanlı	6	6

This comparison further validates the simulation results and underlines the importance of scenario earthquake simulations in seismically active regions. Such studies could investigate the damage potential in future possible earthquakes on active faults. Thus, it is possible to assess localized damage areas even before a large earthquake occurs in a region of interest.

Finally, the simulated intensity distribution is compared to the observed damage distribution of Çay earthquake. As a measure of the building damage in the near-fault area, we define a mean damage ratio (MDR) for each subprovince of Afyon based on damage surveys performed on reinforced concrete residential buildings (Ozmen, 2002). In these damage surveys, each building is classified into one of the following damage states: none (N), light (L), moderate (M), and severe (S) damage cases, and collapse (C) case. Each of these damage states is assigned a central damage ratio which is simply the ratio of the replacement cost of the building to the

original cost of construction (Gurpinar et al., 1978; Askan and Yucemen, 2010) as shown in Table 3.

MDR in a subprovince is then calculated as a weighted average of the occurrence rates of each damage level (discrete probabilities of damage states), where the weights are the central damage ratios. In other words, for a region with no building damage the MDR is 0% and in a region where all the buildings have collapsed the MDR is 100%.

Table 4 lists the number of residential buildings in different damage states for several subprovinces of Afyon. The data is taken from the earthquake report by Ozmen (2002). Table 5 displays the same information in terms of probability of occurrences of damage states and mean damage ratios. Figure 3.30a and Figure 3.30b compare the simulated MMI map with the MDR distribution map. In general, higher levels of simulated intensity correspond to higher MDR values on the maps. There are discrepancies at some subprovinces which are most probably due to the uncertainties in damage data collection in the field as well as approximations in ground motion modeling such as uniform site effects.

Table 6: Definition of damage states and central damage ratios

Damage Level	Definition	Central Damage Ratio (%)
N	No damage	0
L	Light damage	5
M	Moderate damage	30
S	Severe damage	70
C	Collapse damage	100

Table 7: The number of residential buildings in different damage states in Afyon

Town	Total Number of Buildings	Severely Damage-Collapse	Moderate Damage	Light Damage
	2000	Residential	Residential	Residential
Afyon(M)	53416	1116	143	1597
Bayat	2132	9	2	144
Bolvadin	17064	471	436	3163
Çay	11228	1226	136	1660
Çobanlar	2692	445	375	972
İhsaniye	3435	3	0	153
İscehisar	5313	45	3	56
Sandıklı	1460	0	1	10
Sincanlı	3600	35	2	52
Sultandağı	7635	712	302	1427

Table 8: The occurrence rate of different damage states for residential buildings in Afyon

Town	Severely Damage-Collapse	Moderate Damage	Light Damage	MDR
	Residential	Residential	Residential	
Afyon(M)	2.09%	0.27%	2.99%	2.01%
Bayat	0.42%	0.09%	6.75%	0.72%
Bolvadin	2.76%	2.56%	18.54%	4.04%
Çay	10.92%	1.21%	14.78%	10.38%
Çobanlar	16.53%	13.93%	36.11%	20.04%
İhsaniye	0.09%	0.00%	4.45%	0.30%
İscehisar	0.85%	0.06%	1.05%	0.79%
Sandıklı	0.00%	0.07%	0.68%	0.05%
Sincanlı	0.97%	0.06%	1.44%	0.92%
Sultandağı	9.33%	3.96%	18.69%	10.05%

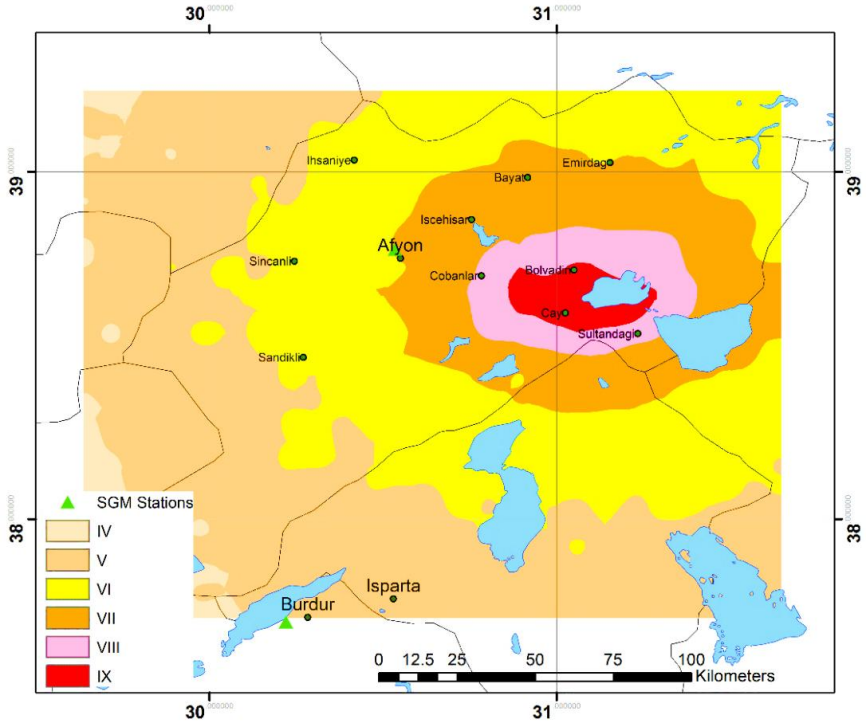

Figure 3.30a: Simulated intensity map of Çay earthquake

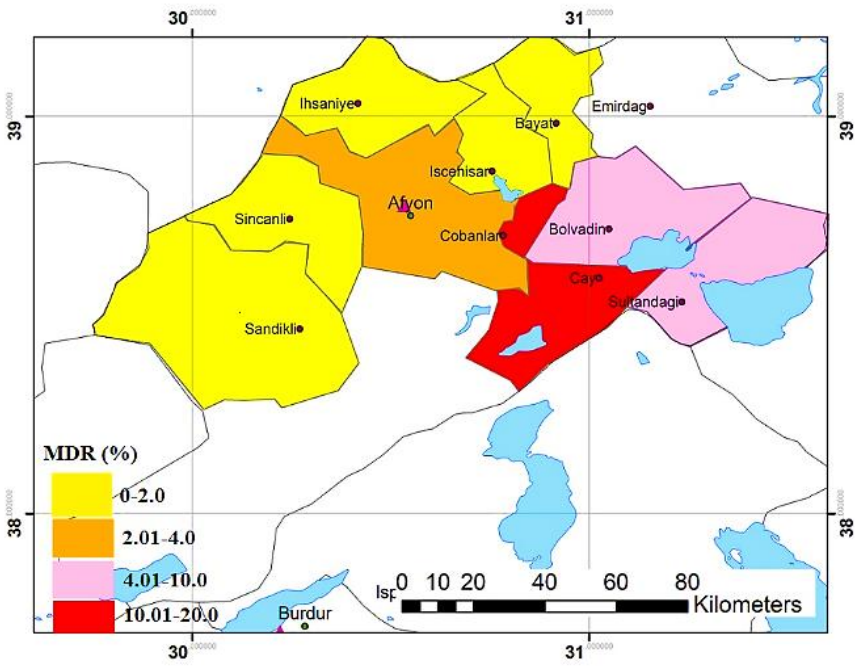

Figure 3.30b: Mean damage ratio distribution after Çay earthquake based on damage data

The comparison of the intensity values for the towns specified in Ozmen's study are shown in Table 9.

Table 9: Comparison of the the simulated MMI with the MDR distribution for Afyon Province

Town	Simulated Intensity	Intensity from MDR
Afyon (M)	6	7
İscehisar	7	6
Bayat	7	6
İhsaniye	6	6
Sandıklı	6	6
Çobanlar	8	9
Sultandağı	8	8
Bolvadin	9	8
Çay	9	9
Sincanlı	6	6

3.6.3 Response Spectra Construction for Engineering Purposes

For design purposes, generally the most common tool to determine the earthquake induced forces that the structures are exposed to, is response spectra analysis. When the structures are regular or investigating the duration effect are less important this type of analysis is performed by most of the engineers. Otherwise, when there is a special type of structure, such as a tall building or historical place then time history analysis should be performed.

In Figure 3.31-3.33, acceleration, velocity and displacement response spectra of the simulated Çay earthquake are shown for 3, 5 and 7% damping values.

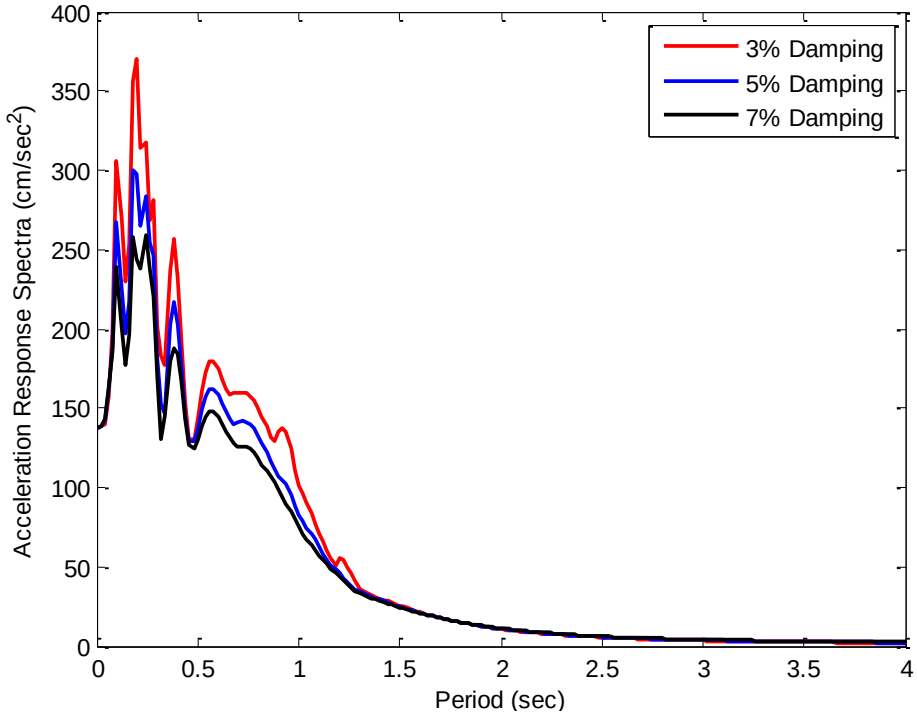

Figure 3.31: Acceleration response spectra from simulated record

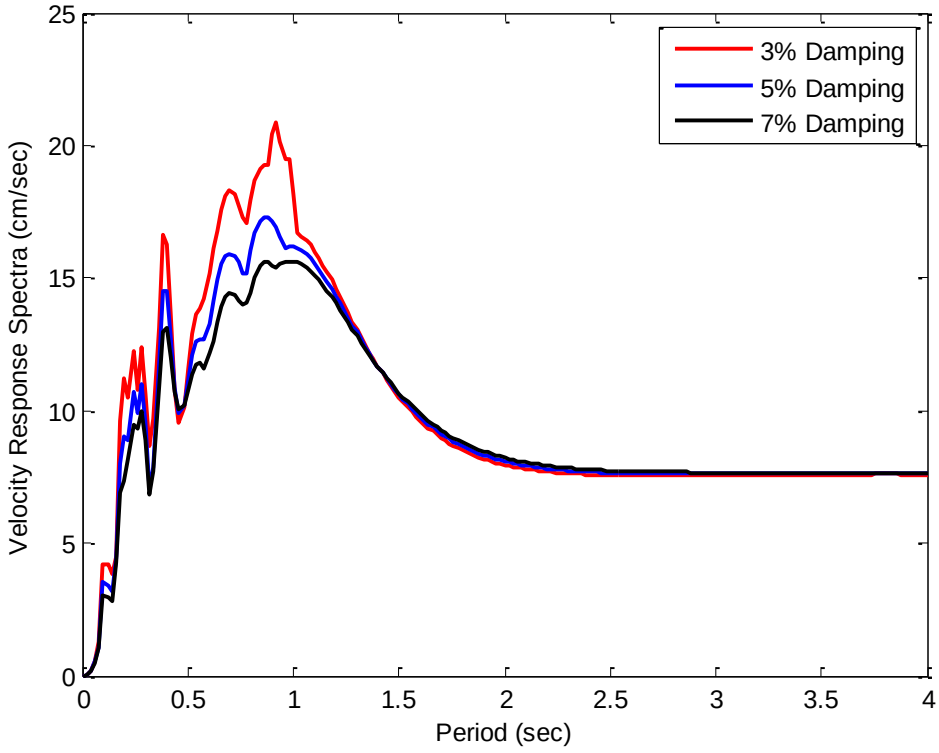

Figure 3.32: Velocity response spectra from simulated record

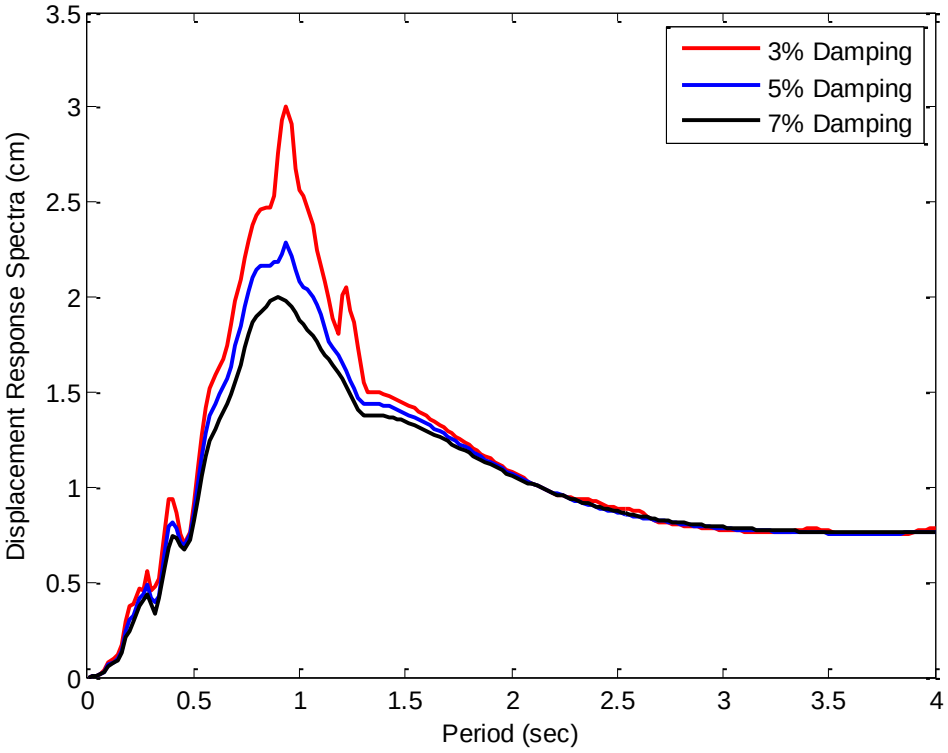

Figure 3.33: Displacement response spectra from simulated record

CHAPTER 4

CONCLUDING REMARKS

4.1 Summary

This study presents the stochastic finite-fault simulation of 3 February 2002 Çay earthquake. The source model is selected from a set of previous studies on the event. Path parameters are adapted from models in previous studies derived with data from the region or other regions with similar seismotectonic settings. Finally, site parameters are derived within this study for each station of interest.

The mainshock is simulated and the model parameters are verified against the scarce recordings in the near-field region. Then, blind simulations are performed for dummy nodes in the epicentral region in order to see the spatial distribution of peak ground motion parameters and to compare the synthetic data with alternative GMPEs from the literature. Lastly, an intensity map is generated from simulated ground motions and compared with the observed intensity map and the damage distributions in the field.

Similar studies can be used for estimating the anticipated ground motion field from large earthquakes at points where there are no stations. In addition, ground motions from scenario events on active faults can also be performed with such modeling techniques.

4.2 Observations and Conclusions

It is well known that in regions of sparse seismic networks or seismic activity with long return periods, simulations become essential. This is particularly true when not only the peak ground motion parameters but the full time series of acceleration is required for earthquake engineering purposes.

In such cases, simulations become essential for reliable seismic hazard estimation, damage mitigation and earthquake resistant design. Ground motion simulations are important not only for providing the peak seismic design parameters but also for offering an understanding of the earthquake mechanisms and the properties of the Earth media in the region of interest.

Following conclusions are drawn directly from the observations in this thesis:

- Stochastic simulations provide reasonable accuracy in validating the individual acceleration records when the model parameters are selected carefully. These simulations provide more physics-based information on time histories generated during large events than the empirical GMPEs that yield only the peak parameters.

- It is well known that near-field records possess complex source effects particularly in low frequencies. During the simulations, it is observed that stochastic method has limitations in modeling the low frequency portions of Fourier amplitude spectra which is believed to be governed by complex source phenomena which the model cannot fully capture.

- An important point is the reliable modeling of the local site response at stations. Site amplification has a direct impact on the duration, frequency content and amplitudes of the ground motions. Consequently, it is essential to assess the local soil conditions and estimate corresponding site response in detail in regions with high seismic hazard.

- The simulated records provide a reasonable match with the synthetics in the frequency range of most engineering interests (>1 Hz). Thus, simulated records could be employed for earthquake engineering purposes after certain validation tests (such as duration and energy content).

- In general, the attenuation of synthetics is observed to match the general characteristics of GMPEs. As a result, in regions of sparse data, synthetic peak ground motion intensity parameters can be used to augment empirical GMPEs. Such an approach would probably yield better results than directly employing a GMPE derived using datasets from elsewhere in the world.

- In this study, simulated peak ground motion values when used in empirical formulae between MMI and PGA/PGV/S_A derived from Turkish data yield intensity distributions consistent with the observed values. This observation is important for future Shakemap (computed intensity map) applications from real or scenario earthquakes which could be used for rapid response, disaster management and overall seismic loss mitigation purposes.

- It is observed that scarcity of recorded data in the near-field region limits the model in terms of validating the input parameters.

4.3 Future Recommendations

- It is important to cover all frequency bands effectively with simulations. Thus, hybrid methods combining deterministic approaches for the lower and stochastic approaches for the higher frequencies must be employed in the future for simulating the large events in Turkey. For this purpose, refined velocity models should be derived for use in full wave propagation studies.

- It is well known that frequency-dependent amplifications directly influence the amplitudes of the ground motion at all frequencies. Thus, improved site amplification models can be developed by using deeper soil profiles (going down to depths greater than 30m) in the theoretical approach. Similarly, whenever available, more data must be employed to increase the accuracy of the empirical H/V method.

- It is possible to use ground motion simulations as input to a variety of studies regarding earthquake engineering. The results can be combined with building fragility functions in order to estimate the loss from potential earthquakes (Ugurhan *et al.*, 2011); employed in nonlinear dynamic analyses of building structures (Karimzadeh et al., 2014) or can be used to derive fragility functions based on regional seismicity directly. Further tests with simulated data versus real ones will lead to new research ideas at the intersection of seismology and engineering.

- Almost all the model parameters and efficiency of the simulations depend on the amount of high-quality data in seismically active regions. As of now, there are still many regions in the world and in our country without sufficiently dense networks. Thus, for better assessment of seismicity in such regions, it is significant to increase the number of strong ground motion stations under operation and widen the seismic networks all over the world and particularly in our country.

- This study and similar studies can be further developed and employed to assess potential ground motions in anticipated earthquakes. Thus, necessary measures can be taken prior to large events to minimize future seismic losses in general.

REFERENCES

Abrahamson, N. A., and W. J. Silva (2008). Summary of the Abrahamson & Silva NGA Ground-Motion Relations, *Earthquake Spectra* **24**, 67-97.

Aki, K. (1967). Scaling law of seismic spectrum, *J. Geophys. Res.* **72,** 1217–1231.

Aki, K. (1980). Attenuation of shear waves in the lithosphere for frequencies from 0.05 to 25 Hz, *Phys. Earth Planet. Inter.*, **21**, 50-60.

Aki, K. and P. G. Richards (1980). Quantitative Seismology, W. H. Freeman and Co., San Francisco, 932 pp.

Akinci, A., J.M. Ibáñez, E. del Pezzo, J. Morales (1995). Geometrical spreading and attenuation of Lg waves: a comparison between western Anatolia (Turkey) and southern Spain, *Tectonophysics* **250**, 47-60.

Akinci, A., S. D'Amico, L. Malagnini, A. Mercuri (2013). Scaling earthquake ground motions in western Anatolia, Turkey, *Physics and Chemistry of the Earth* **63**, 124-135.

Akkar S, MA Sandıkkaya, JJ Bommer (2013). Empirical ground-motion models for point- and extended-source crustal earthquake scenarios in Europe and the Middle East, *Bulletin of Earthquake Engineering*, ISSN: 1570-761X

Aktug, B., B. Kaypak, R. N. Celik (2009). Source parameters for the Mw = 6.6, 03 February 2002, Çay Earthquake (Turkey) and aftershocks from GPS, Southwestern Turkey, *Journal of Seismology* **14**, 445-456.

Anderson, J. and S. Hough (1984). A model for the shape of the Fourier amplitude spectrum of acceleration at high frequencies, *Bull. Seism. Soc. Am.* **74,** 1969–1993. 106

Askan, A. and M. S. Yucemen (2010). Probabilistic Methods for the Estimation of Potential Seismic Damage: Application to Reinforced Concrete Buildings in Turkey, *Structural Safety* **32**, 262-271

Askan, A., F. N. Sisman, B. Ugurhan (2013). Stochastic strong ground motion simulations in sparsely-monitored regions: A validation and sensitivity study on the 13 March 1992 Erzincan (Turkey) earthquake, *Soil Dynamics and Earthquake Engineering* **55**, 170-181.

Askan, A., F. N. Sisman, O. Pekcan (2014). A Regional Near-Surface High Frequency Spectral Attenuation (Kappa) Model for Northwestern Turkey, *Soil Dynamics and Earthquake Engineering* (under revision).

Atkinson, G. M and W. Silva (2000). Stochastic Modeling of California Ground Motions, *Bull. Seism. Soc. of Am.* **90**; 255-274.

Atkinson, G. (2004). Empirical attenuation of ground motion spectral amplitudes in southeastern Canada and the northeastern United States, *Bull. Seism. Soc. Am.* **94,** 1079 –1095.

Atkinson, G. M., K. Assatourians, D. M. Boore, K. Campbell and D. Motazedian (2009). A Guide to Differences between Stochastic Point-Source and Stochastic Finite-Fault Simulations, *Bull. Seism. Soc. Am*. **99,** 6, 3192–3201.

Beresnev, I. and G. M. Atkinson (1997). Modeling finite-fault radiation from the n spectrum, *Bull. Seism. Soc. Am.* **87**, 67 - 84. 107

Beresnev, I. and G. M. Atkinson (1998a). FINSIM—a FORTRAN program for simulating stochastic acceleration time histories from finite-faults, *Seism. Res. Lett.* **69,** 27–32.

Beresnev, I. and G. M. Atkinson (1998b). Stochastic finite-fault modeling of ground motions from the 1994 Northridge, California earthquake. I. Validation on rock sites, *Bull. Seism. Soc. Am.* **88,** 1392–1401.

Bilal, M. and A. Askan (2014). Relationships between felt intensity and recorded ground motion parameters for Turkey, *Bulletin of the Seismological Society of America* 104, 1, 484–496.

Boore, D. M. (1983). Stochastic simulation of high-frequency ground motions based on seismological models of the radiated spectra, *Bull. Seism. Soc. Am.* 73, 1865–1894.

Boore, D.M. and W.B. Joyner (1997). Site amplifications for generic rock sites, *Bull. Seism. Soc. Am.* 87, 327–341.

Boore, D. M. (2003). Simulation of ground motion using the stochastic method, *Pure and Applied Geophysics* 160, 635-675.d

Boray A, ¸F. Şaroğlu F, Ö. Emre (1985). Evidence for E-W shortening in the north of Isparta Angle, *Jeoloji Mühendisliği* **23**, 9–20.

Bouchon, M. (1978). A dynamic source model for the San Fernando earthquake, *Bulletin of Seismological Society of America* **68**, 1555-1576.

Brune, J. (1970). Tectonic stress and the spectra of seismic shear waves from earthquakes, *J. Geophys. Res.* **75,** 4997–5009.

Brune, J. (1971). Correction, *J. Geophys. Res.* **76,** 5002.

Castro, R.R., F. Pacor, G. Franceschina, D. Bindi, G. Zonno, and L. Luzi (2008). Stochastic Strong-Motion Simulation of the Mw 6 Umbria–Marche Earthquake of September 1997: Comparison of Different Approaches, *Bull. Seism. Soc. Am.* **98**, 662–670.

Chen, X. and Zhang H. (2001). An Efficient Method for Computing Green's Functions for a Layered Half-Space at Large Epicentral Distances, *Bull. Seism. Soc. Am.* **91,** 858 - 869.

Chiou, B. S.-J. and R. R. Youngs (2008). An NGA model for the average horizontal component of peak ground motion and response spectra, *Earthquake Spectra* **24**, 173-215.

Claprood, M. And Asten, M. (2009). Initial results from spatially averaged coherency, frequency-wavenumber, and horizontal to vertical spectrum ratio microtremor survey methods for site hazard study at Launceston, *Exploration Geophysics* **40**, 132–142.

Douglas, J., P. Gehl, L. F. Bonilla, C. Gelis (2010). A κ model for mainland France, *Pure and Applied Geophysics* **167**, 1303-1315.

Erberik, M.A. (2008a). Generation of fragility curves for Turkish masonry buildings considering in-plane failure modes, *Earthquake Engineering and Structural Dynamics* **37**, 387-405.

Erberik, M.A. (2008b). Fragility-based assessment of typical mid-rise and low-rise RC buildings in Turkey, *Engineering Structures* **30**, 1360-1374.

Ergin, M. M. Aktar, S. Ozalaybey, M. C. Tapirdamaz, O. Selvi, A. Tarancioglu (2009). A high-resolution aftershock seismicity image of the 2002 Sultandağı-Çay earthquake (Mw=6.2), Turkey, *Journal of Seismology* **13**, 633-646.

Faenza, L. and A. Michelini (2010). Regression Analysis of MCS Intensity and Ground Motion Parameters in Italy and its Application in ShakeMap, *Geophysical Journal International* **180**, 1138-1152.

Galuzzo, D., G. Zonno and E. Del Pezzo (2008). Stochastic Finite-Fault Ground-Motion Simulation in a Wave-Field Diffusive Regime: Case Study of the Mt. Vesuvius Volcanic Area, *Bull. Seism. Soc. of Am.* **98**; 1272-1288.

Gurpinar A, M. Abalı, M. S. Yucemen, Y. Yesilcay (1978). Feasibility of mandatory earthquake insurance in Turkey. *Earthquake Engineering Research Center, Middle East Technical University, Ankara*, Report No. 78-05.

Hanks, T. C. and R. K. McGuire (1981). The character of high frequency strong ground motion, *Bull.Seism. Soc. Am.* **71**, 2071-2095.

Hanks, T. C. (1982). fmax, *Bull.Seism. Soc. Am.* **72**, 1867-1879.

Hartzell, S. (1978). Earthquake aftershocks as Green's functions, *Geophys. Res. Lett.* **5**, 1–14.

Haskell, N. A. (1964). Total energy and energy spectral density of elastic wave radiation from propagating faults, *Bull. Seism. Soc. Am.* **54**, 1811-1841.

Herrmann, R.B. (1985). An extension of Random Vibration Theory estimates of strong ground motion to large earthquakes, *Bull. Seis. Soc. Am.* ***75,*** 1447–1453.

Hisada, Y. (2008). Broadband strong motion simulation in layered half-space using stochastic Green's function technique, *Journal of Seismology*, **12**, 265-279.

Housner, G. W. (1947). Characteristics of strong-motion earthquakes, *Bull. Seis. Soc. Am.* **37,** 19 - 31.

Housner, G. W. (1955). Properties of strong ground motion earthquakes, *Bull. Seis. Soc. Am.* **45,** 197 – 218.

Karimzadeh, S., A. Askan, A. Yakut and G. Ameri (2014). Nonlinear Time History Analyses of Structures Under Real and Synthetic Ground Motions, *Journal of Earthquake Engineering* (under revision).

Kocyigit, A., E. Unay, G. Sarac, G. (2000). Episodic graben formation and extensional neotectonic regime in West Central Anatolia and the Isparta Angle: a case study in the Akşehir-Afyon Graben, Turkey. *Geological Society, London, Special Publications* **173**, 405-421.

Kocyigit A., E. Bozkurt, N. Kaymakci, F. Saroglu (2002). Source Mechanism of 3 February 2002 Çay (Afyon) Earthquake and Damage Reasons: Akşehir Fault Zone, Geo. Preliminary Report, *Middle East Technical University Faculty of Engineering Geological Engineering Tectonics Research Unit* (in Turkish).

Kramer, S.L. (1996). Geotechnical Earthquake Engineering, Prentice Hall, Inc., Upper Saddle River, New Jersey, 653 pp.

Lachet, C., and P.Y. Bard (1994). Numerical and theoretical investigations on the possibilities and limitations of the Nakamura's technique, *Journal of Physics of the Earth* **42**, 377–397.

McGuire, R. K. and T. C. Hanks (1980). RMS accelerations and spectral amplitudes of strong ground motion during the San Fernando, California, earthquake, *Bull. Seism. Soc. Am.* **70,** 1907–1919.

Mohammadioun, B. and L. Serva (2001). Stress drop, slip type, earthquake magnitude, and seismic hazard, *Bull. Seismol. Soc. Am.* **91,** 694–707.

Motazedian, D., and G. M. Atkinson (2005). Stochastic finite-fault modeling based on a Dynamic Corner Frequency, *Bull. Seism. Soc. Am.* **95,** 995–1010.

Motazedian, D. (2006). Region-specific key seismic parameters for earthquakes in northern Iran, Bull. Seismol. Soc. Am. **96**, 1383–1395.

Motazedian, D. and A. Moinfar (2006). Hybrid stochastic finite fault modeling of 2003, M6.5, Bam earthquake (Iran), *Journal of Seismology* **10**, 91-103.

Nakamura, Y. (2008). On the H/V Spectrum, *the 14th World Conference on Earthquake Engineering.*

Ozden, S., K. S. Kavak, F. Kocbulut, S. Over, H. Temiz (2002). February 3, 2002 Çay (Afyon) Earthquakes, *Türkiye Jeoloji Bülteni* **45**. (in Turkish)

Ozer, N., Y. Altınok, M. Utkucu, E. Yalcinkaya, O. Alptekin, A. Pınar, A. I. Kanlı, S. Şahin (2002). Observations and Evaluations of the February 3, 2002 Afyon (Çay-Eber) Earthquake, *Yerbilimleri Dergisi* **15**, 11-24. (in Turkish)

Ozmen, B. (2002). Seismic intensity map and damage distribution of 3 February 2002 Çay (Afyon) earthquake, Directorate of Disaster Affairs, Ankara, Report No: 4083.1 (in Turkish).

Tokimatsu, K., (1997) Geotechnical site characterization using surface waves: in Ishihara (ed.). *Earthquake Geotechnical Engineering*, Balkema.

Papageorgiou, A. S. and K. Aki (1983). A specific barrier model for the quantitative description of inhomogeneous faulting and prediction of strong ground motion, Part I and II, *Bull. Seis. Soc. Am.* **73**, 693-722 and 953-978.

Pitarka, A., K. Irikura, K. Kamae (1998). A Technique for Simulating Strong Ground Motion Using Hybrid Green's Function, *Bulletin of Seismological Society of America* **88**, 357-367.

Raghukanth, S. T. G. and S. N. Somala (2009). Modeling of Strong-Motion Data in Northeastern India: Q, Stress Drop, and Site Amplification, *Bull. Seism. Soc. Am*. **99**, 705-725.

Roumelioti, Z., A. Kiratzi, and N. Theodulidis (2004). Stochastic Strong Ground-Motion Simulation of the 7 September 1999 Athens (Greece) Earthquake, *Bull. Seism. Soc. Am.* **94**, 1036 - 1052.

Sanchez-Sesma, F.J. (1987). Site effects on strong ground motion, *Soil. Dyn. Earthq. Eng.* **6**, 124-132. Schmidt, R.O. (1986). Multiple emitter location and signal parameter estimation. IEEE Transactions on Antennas and Propagation, AP-34, 276-280.

Saragoni, G. R. and G. C. Hart (1974). Simulation of artificial earthquakes, *Earthquake Engineering and Structural Dynamics* **2**,249-267.

Scherbaum, F., Hinzen, K.-G. & Ohrnberger, M. (2003) Determination of shallow shear wave velocity profiles in the Cologne, Germany area using ambient vibrations, *Geophys. J. Int.* **152**, 597-612.

Schnabel, P.B., J. Lysmer, Seed, H. Bolton (1972). SHAKE: A Computer Program for Earthquake Response Analysis of Horizontally Layered Sites. *Earthquake Engineering Research Center, University of California Berkeley 72*, 102.

Shoja-Taheri, J., and H. Ghofrani (2007). Stochastic Finite-Fault Modeling of Strong Ground Motions from the 26 December 2003 Bam, Iran, Earthquake, *Bull. Seism. Soc. Am.* **97**, 1950 - 1959.

Silva, W.J., and K. Lee (1987). "WES RASCAL code for synthesizing earthquake ground motions." State-of-the-Art for Assessing Earthquake Hazards in the United States, *U.S. Army Engineers Waterways Experiment Station, Misc*. **24** , 73-1.

Stein, S. and M. Wysession (2003). An Introduction to Seismology, Earthquakes, and Earth Structure, Blackwell Science, Oxford, 498 pp.

Strong Ground Motion Database of Turkey, DAPHNE, http://daphne.deprem.gov.tr:89/2K/daphne_v4.php, last visited on 15 February 2014.

Saroğlu, F., O. Emre, A. Boray (1987). Seismicity and active faults of Turkey, *General Directorate of Mineral Research and Exploration Report No. 8174* (in Turkish)

Taymaz T., O. Tan (2001). Source parameters of June 6, 2000 Orta–Çankırı (Mw=6.0) and December 15, 2000 Sultandağı–Akşehir (M_w=6.0) earthquakes obtained from inversion of teleseismic P- and SH body-waveforms. *Symposia on Seismotectonics of the North-western Anatolia–Aegean and recent Turkish earthquakes, Atlas*, 96–107.

Toro, G. R. and R. K. McGuire (1987). An Investigation into Earthquake Ground Motion Characteristics in Eastern North America, *Bull. Seismol. Soc. Am.* **77**, 468–489.

Thomson, W. T. (1959). Spectral Aspect Of Earthquakes, *Bull. Seism. Soc. Am.* **49**, 91-98.

Ugurhan, B. and A. Askan (2010). Stochastic Strong Ground Motion Simulation of the 12 November 1999 Düzce (Turkey) Earthquake Using a Dynamic Corner Frequency Approach, *Bull. Seism. Soc. Am.* **100**, 1498-1512.

Ugurhan, B., A. Askan and M.A. Erberik (2011). A Methodology for Seismic Loss Estimation in Urban Regions Based on Ground Motion Simulations, *Bulletin of the Seismological Society of America* **101**, 710–725.

Ugurhan, B., A. Askan, A. Akinci, L. Malagnini (2012). Strong-Ground-Motion Simulation of the 6 April 2009 L'Aquila, Italy, Earthquake, *Bulletin of the Seismological Society of America* **102**, 1429-1445.

Ulusay, R., Ö. Aydan, A. Erken, E. Tuncay, H. Kumsar, Z. Kaya (2004). An overview of geotechnical aspects of the Çay-Eber (Turkey) earthquake, *Engineering Geology* **73**, 51-70.

Utku M., M. Danışman, N. Akyol N, Z. Akçığ (2003). The seismicity of Afyon and its surroundings: isoseist map of 03 February 2002 Çay Earthquake, and earthquake risk analysis, *Geol. Eng.* **27.**

Wald, D.J., V. Quitoriano, T.H. Heaton, H. Kanamori, C.W. Scrivner, and B.C. Worden (1999a). TriNet "ShakeMaps": Rapid generation of peak ground-motion and intensity maps for earthquakes in southern California, *Earthquake Spectra* **15**, 537-556.

Wells, D., and K. Coppersmith (1994). New empirical relationships among magnitude, rupture length, rupture width, rupture area, and surface displacement, *Bull. Seism. Soc. Am.* **84,** 974 -1002.

Yalcinkaya, E. (2005). Stochastic Finite-fault Modeling of Ground Motions from the June 27, 1998 Adana-Ceyhan Earthquake, *Earth Planets Space* **57**,107–115.

Yucemen, M. S. and A. Askan (2003). Estimation of earthquake damage probabilities for reinforced concrete buildings, In: S. T. Wasti and G. Ozcebe (eds), Seismic Assessment and Rehabilitation of Existing Buildings, NATO Science Series IV: Earth and Environmental Sciences, Kluwer Academic Publishers, **29**, 149–164.